Decreasing Error in Functional Hip Joint Center Calculation using Ultrasound Imaging

Swati Upadhyaya

Thesis submitted to the

Faculty of Graduate and Postdoctoral Studies

In partial fulfillment of the requirements for the degree

Master of Applied Science in Biomedical Engineering

Ottawa-Carleton Institute for Biomedical Engineering

School of Information Technology and Engineering

University of Ottawa

Ottawa, Ontario, Canada

May 2013

Abstract

The hip joint center (HJC) is needed for calculation of hip kinematics in various applications. In the functional method, the center is determined by moving femur with respect to acetabulum. A popular way for measuring this movement is through an optical motion capture system. This method is fast and economical for most applications where we require an instant HJC even though the reconstruction error in bone position calculation exists due to skin artifact. This error is caused by movement of markers placed on skin rather than on actual bone. Here we introduce ultrasound imaging as an additional modality to measure the change in soft tissue thickness above bone while hip is flexed. We use this information on the tissue thickness change to recalculate position of markers placed on skin to match the movement of bone. A good advantage of using ultrasound machine is its non-invasiveness. We calculated HJC using a symmetric center of rotation estimation (SCoRE) algorithm, which uses the concept of coordinate transformation on 3D marker position data. The algorithm gives the 3D position of two centers, one for each hip bone. The distance between these two centers (SCoRE residual) gives us a hint on the accuracy of the HJC calculation and has been proved to be proportional to the error with respect to actual center in previous studies. These two centers should ideally coincide as they collectively form a spherical joint. Our new algorithm for HJC calculation with tissue thickness compensation, measured using ultrasound imaging shows the error has been reduced from *9.13 mm* to *4.87 mm*.

Acknowledgments

I wish to extend my sincere gratitude to the people without whom it would not have been possible for me to sail through this journey towards completion of Master's Degree program. First and foremost I would like to extend my gratefulness towards my research supervisor, Dr WonSook Lee whose invaluable time and guidance at each stepping stone has come in handy to develop myself as a professional. She has a major hand for my achievements throughout the past 2 years. I would also like to thank Dr. Chris Joslin and Dr. Yuu Ono for providing their essential lab equipment and guidance which has made this work successful along with Mr. Zhen Qu's extensive support. I am also thankful to my lab mates and coworkers for maintaining a warm work environment in the lab.

This would be incomplete without mentioning my father, Mr Lakshmi Shanker Upadhyaya and my mother Mrs Gayatri Devi, who took courage to send me abroad and I thank them for keeping faith in me. I would like to thank my dear friend, Mr Prerak Dharia, who constantly encouraged and supported me throughout my stay in Ottawa. Very special thanks to Dr. T. Murty and his wife Mrs Kamla Murty who made my stay in Ottawa a pleasant experience to be remembered forever. This would not be complete without mentioning Miss Ritishka Grover, who provided an amazing support system as a roommate and friend.

I would also like to thank the National Science and Engineering Research of Canada for funding the Collaborative Health Research Project "Detection and Simulation of Femoroacetabular Impingement" to help me carry out the research on the topic.

Table of Contents

List of Figures and Tables

Chapter 1. Introduction

Hip joint center (HJC) is the center of rotation of the human hip joint. This center is needed as a reference point in various applications for various purposes. In applications such as human gait analysis, this center is needed for calculation of hip joint kinematics and kinetics such as hip joint angle, range of motion, hip moment and torque generated by surrounding muscles. HJC is used as a reference point for medical applications such as navigation based surgical systems, prosthetic alignment and bone reduction surgeries for certain joint abnormalities [55].

This hip joint center can be calculated through various methods ranging from static geometric shape analysis of joint anatomy or through analysis of dynamic hip motion. In shape based methods, the medical images such as MRI or CT scan of hip joint is examined by an expert who determines the stationary joint center through geometric analysis. Another way to calculate the center is to use information regarding distances between certain points on hip such a bony landmarks to use statistical shape analysis and predictive regression modeling to calculate the center. Motion based approach to calculate HJC is commonly known as functional method. This widely used method in gait laboratories and surgical navigation systems gives HJC within a decent accuracy when compared to the geometric center. In the functional method it is assumed that human hip is a ball and socket joint. Markers are placed on thigh and pelvis such that their three dimensional (3D) position can be recorded. Thigh is moved in various non-planar movements like flexion, extension, abduction, adduction and circumduction with respect to pelvis. The movement of femur is then measured relative to pelvis through these external markers placed on body and HJC is

calculated from the obtained marker trajectories in 3D through established algorithms. This method is more convenient and in-expensive compared to shape analysis of medical images and more accurate than prediction methods based on regression modeling.

Here we are interested in improving the calculation of center of rotation of the hip through functional methods. Hence we analyze the existing algorithms and the major source of error through literature review while concentrating on ways to improve this method for increasing accuracy of HJC calculation.

1.1 Problem Statement

In optical human motion analysis experiments, markers are placed on the body so that its movement can be recorded as 3D position of marker trajectory through special cameras. Markers placed on the surface of the body (skin) are not rigidly attached to the underlying bone. The algorithms used for reconstruction of bone position through external markers assume that these markers are rigidly attached with the bone, even during the motion. In fact, the underlying bone does not remain stationary with respect to the skin while the hip is moved and hence this assumption does not hold true. While the bone does not remain in center compared to the overlying skin due to contraction and relaxation of muscles when the hip is moved, its reconstruction from markers placed on skin does not represent the true bone position.

The method of finding HJC through motion analysis of hip joint based on positions of external markers suffers from a source of error termed as soft tissue artifact (STA). The error is measured as distance between the calculated center and the true center (available through MRI/CT images). This error is caused due to displacement of markers placed on skin with

respect to underlying bone when specific movements like flexion, extension, abduction, adduction and circumduction are made.

This displacement of markers poses problems in reconstructing accurate bone positions using existing algorithms and leads to an error of up to *14 mm* [43] in calculating HJC. Studies have been carried out to measure the displacement of skin markers with respect to a bone rigid frame of reference. This local frame of reference rigidly attached to bone is achieved by recording the movement of markers placed on pins which can be inserted in bone. Nonetheless, this is an invasive procedure and not feasible to apply on live humans. Soft tissue artifact has been found out to be dependent on task being carried out (type of movement), subject's body attributes and location of markers on the segment of body [16].

Due to subject specific nature of this error, a general mathematical model based correction established on previous experiments is not applicable to other studies. Hence there appeared a need to track and compensate this error during the experiment for each participant as an adhoc exercise. Existing methods are invasive and therefore not feasible to be applied in either gait laboratories or navigation based surgical applications for live humans.

Consequently, it was desired to develop a non-invasive system to improve the reconstruction of the bone position from markers placed on skin to improve motion analysis based functional hip joint center calculation.

1.2 Ultrasound as an Ad hoc Modality

Ultrasound is a portable and non-invasive imaging modality that can give real time measurement of depth of bone position through a set of images. Bone is visible as a contrast in the image due to its dense nature compared to the surrounding tissues.

There exists a need to accurately reconstruct the underlying bone movement from markers placed on skin. We sought a way to track the trajectory of bone on thigh by integrating ultrasound imaging with an optical motion capture system. Ultrasound system has been integrated with motion capture systems such as VICON [44] to get a global frame of reference for the image plane and reconstruct a 3D model from 2D images through calibration methods [45]. Recently Sangeux et al. [30] used ultrasound combined with VICON to get a gold standard data for functional hip joint center with *4 mm* accuracy compared to MRI.

Hence, there seemed a possibility to integrate the two systems; Ultrasound and optical motion capture (VICON), to simultaneously track the movement of bone along with the movement of markers on skin. With the motivation of tracking the marker displacement with respect to underlying bone non-invasively, we thought of using ultrasound imaging to measure the change in thickness of tissue underlying the skin on which markers are placed for functional HJC calculation and synchronizing it with the motion capture system to get a bone fixed frame of reference. With this information we aimed to recalculate the marker's position on thigh to better match the trajectory of underlying bone

1.3 Proposed Solution

Based on the literature we found that attempts have been made to reduce soft tissue artifact through linear statistical models or through shape analysis techniques [23]. Although, the error is specific to the participant and cannot be generalized, hence there is a need to evaluate this error every time motion analysis is used to determine the hip joint center to ensure accuracy.

For HJC calculation through motion analysis, markers are placed on thigh and pelvis and thigh is moved with respect to pelvis to record marker trajectory. Our observation was that when the thigh moves the layer of muscle from skin up to bone contracts and relaxes. This changes the muscle thickness and thigh shape. This would affect the distance between markers placed on skin and the underlying bone. This distance would remain constant throughout the motion if the marker on skin was rigidly attached to the bone and marker position on skin could represent the position of underlying bone.

We propose the idea of observing the change in distance between the bone and skin. This information on depth of bone can be obtained from ultrasound imaging. Simultaneously, we capture the position of markers placed on thigh and pelvis for calculation of HJC through a motion capture system (VICON). We also track the position of ultrasound probe in 3D space by placing markers on it. Hence by synchronizing the two imaging systems we can get an estimate of the position of bone in 3D space. The markers on probe allow us to have a probe's rigid frame of reference that moves rigidly with the thigh. Position and orientation of the frame of reference attached to thigh calculated with markers on skin are then adjusted using this information to give a trajectory in 3D which better represents bone motion. Functional HJC calculation is done using coordinate transformation and error is expressed as the difference between calculated pelvic and femur centers. This error value should decrease with our proposed technique and the center should be closer to the actual HJC.

One of the main aims of this research is to track the bone (femur) movement with respect to skin through ultrasound with simultaneous measurement of position of thigh with respect to pelvis and synchronize it with a motion capture system to track the displacement of skin markers with respect to underlying bone. This is an attempt towards assessing and

compensating for soft tissue artifact in a non-invasive manner through a possible ad hoc exercise using ultrasound to model the subject specific and activity specific traits of marker motion.

The second aim of the research is to evaluate the coordinate transformation algorithm SCoRE [20] through the trajectories made by markers on skin to find out hip joint center. The algorithm has a widespread use in gait laboratories to determine functional HJC. Although its accuracy on simulation based experiments has been shown to give an error less than *1 mm*, when it is applied on human based experiments, the error tends to increase by more than ten times [30]. Hence using this algorithm for different experiment settings than those on which the accuracy has been reported might be misleading.

We have applied this algorithm on the 3D coordinate data from markers on skin (thigh and pelvis) to get the position of the center. Then we calculated new 3D positions of marker with the bone trajectory obtained using ultrasound imaging and compared its result with skin marker based calculation to see the improvement. We have made an attempt to accommodate the error due to displacement of skin markers during motion because of change in tissue thickness from skin up to the bone. By translating the markers on skin by the amount of tissue thickness towards bone, we aimed to reconstruct the marker trajectory as it would be when markers were placed directly on bone and hence get a better estimate of hip joint center through existing algorithms.

1.4 Overview of the Document

This document consists of six chapters. The introduction in Chapter 1 provides a broad overview of the problem statement and the proposed solution. As the entity in concern is the

hip joint, in Chapter 2 we have detailed the morphology and physiology of hip joint; the literature review on methodology for hip joint center calculation and details on the algorithms and studies conducted for functional HJC calculation. Chapter 3 links the literature with our research by providing an overview of methodology of our experiments formed on the grounds of previous research and established algorithms. In Chapter 4 we describe the experimental setup, techniques, procedure and equipment used for the experiments. Chapter 5, we have detailed the exploratory analysis of the ultrasound imaging and motion capture data along with the result of HJC derived through markers on skin and compared with the result obtained from the bone trajectory incorporated new calculated marker positions. Chapter 6 concerns the discussion, limitations and future work on the topic. We have presented preliminary results of this thesis in three conferences and in the process of submitting an article for publishing in a Journal.

Chapter 2. Literature Review

2.1 Hip Joint: A Ball and Socket Joint

Hip joint is the anatomical landmark in human body which connects the lower limb bone femur and the abdominal bone acetabulum. The joint is modeled in biomechanical studies as a ball and socket joint [1].

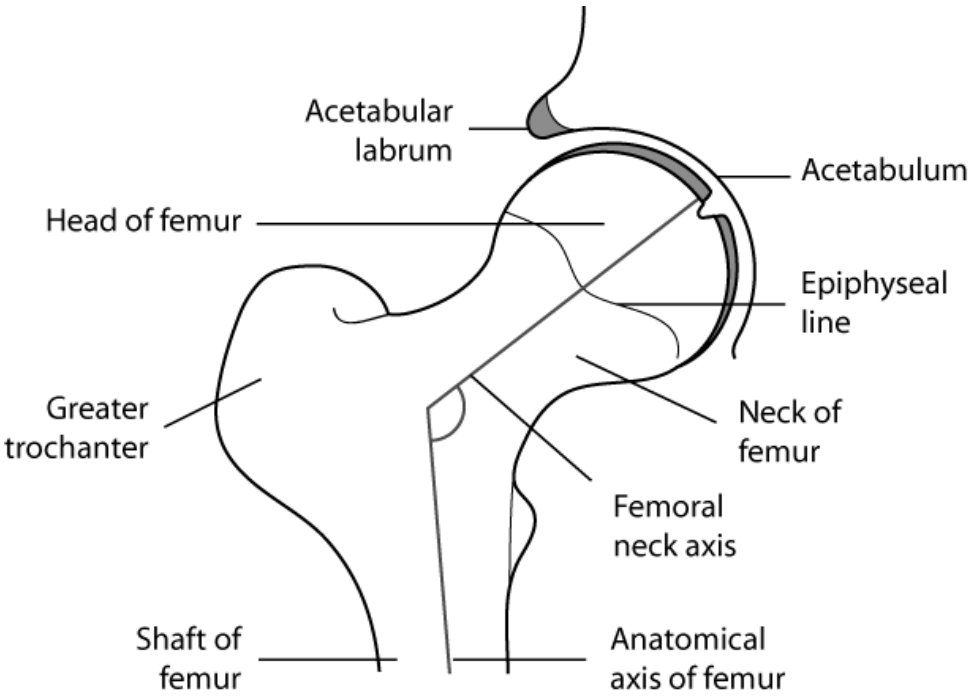

Figure 2.1 Human hip joint anatomy [3]

2.1.1. Anatomy

The anatomy of hip consists of bones, muscles and ligaments. Two major bony parts of hip joint are the thigh bone, Femur and the pelvic bone, Acetabulum [4]. The main parts of these two bones for the joint are described here.

Acetabulum

The proximal part of human hip bone consists of acetabulum which is collectively formed by the fusion of three bones namely ilium, ischium and pubis. The Ilium consists of anterior and posterior iliac spines which are used as anatomical landmarks through palpation. The Ischium is the lower bony part of acetabulum which bears the load of human body in seated positions. The Pubis forms the anterior region of pelvis where the Ilium and Ischium fuse to form the Acetabulum at pubic symphysis. The opening between ischium and pubis is called Obturator Foramen. The Acetabulum contains a cavity opening to accommodate femoral head and is supported by cartilaginous covering, ligaments and the acetabula labrum which serves the purpose of providing a cushion surface to cater the forces around the joint and protect the synovial fluid from flowing into the nearby parts [3] .

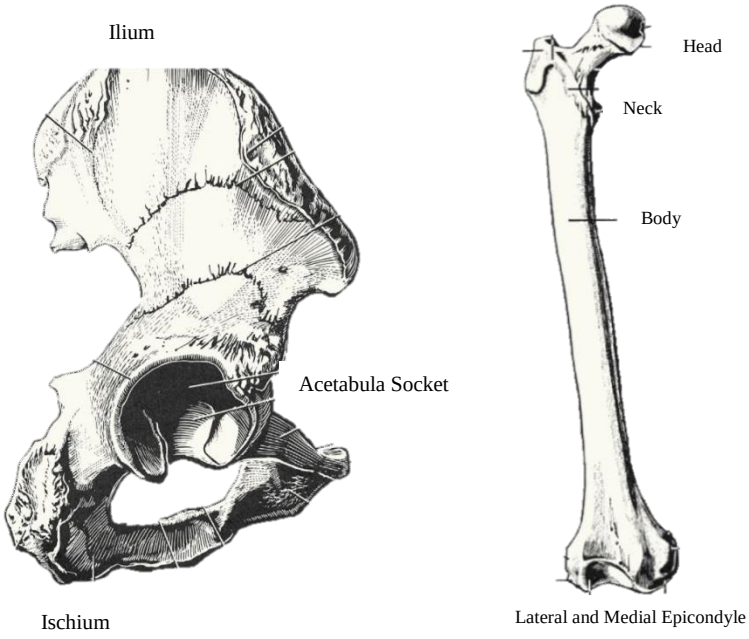

Figure 2.2 Lateral view of right acetabular bone and anterior view of femur [8]

Femur

The distal end of the hip joint consists of the longest and heaviest bone in human body known as Femur [8]. Going from top to bottom, the main parts of femur consists of femur head, neck, greater and lesser trochanter ,body, medial and lateral epicondyle as shown in figure 2.2 The greater trochanter, medical and lateral epicondyles are the palpable bony landmarks for femur [4]. The femur head fits into acetabula cup in order to form the Joint [6]. The neck makes an angle inclined with the head.

The joint is subdivided into three compartments namely anterior, medial and posterior which consists of muscles like rectus, abductor and hamstrings responsible for the strength and functionality of the joint. The arteries and nerves control the blood flow and transmission of signals to the limb.

2.1.2. Physiology

The main function of the Hip joint is to connect the upper trunk of the body from head to abdomen to the lower limbs [6]. This joint bears the weight of the upper body and distributes the load from sacrum to the acetabula while standing. The auto lock mechanism of hip joint enables minimum effort to be put on by the supporting muscles while standing so the center of mass lies posterior to the hip joint and an upright posture is obtained with the help of Illiofemoral ligament. The locomotion functionality of human body is due to the flexible joint rotation which allows for humans to walk. During walking the flexion angle of rotation might reach up to 35° for people without any abnormalities [56]. Due to the lifetime functionality of bearing weight and working against forces, the joint tends to degrade most often with aging.

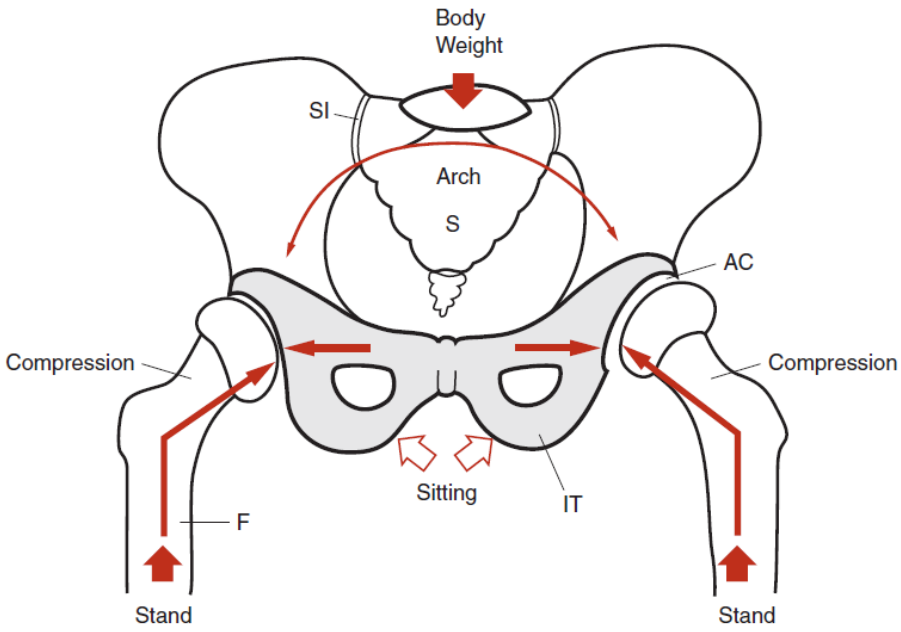

Figure 2.3 Functional anatomy of hip joint showing load bearing points in sitting and standing position [10]

Ball and socket Joint

According to a definition by Britannica Online academic edition, the ball-and-socket joint is defined as "Ball and socket Joint also called spheroidal joint, in vertebrate anatomy, a joint in which the rounded surface of a bone moves within a depression on another bone, allowing greater freedom of movement than any other kind of joint. It is most highly developed in the large shoulder and hip joints of mammals, including humans, in which it provides swing for the arms and legs in various directions and also spin of those limbs upon the more stationary bones."[7]. A perfect spherical joint would have access to move freely without any limits but the human ball and socket joint motion is restricted with many limitations for stability and support.

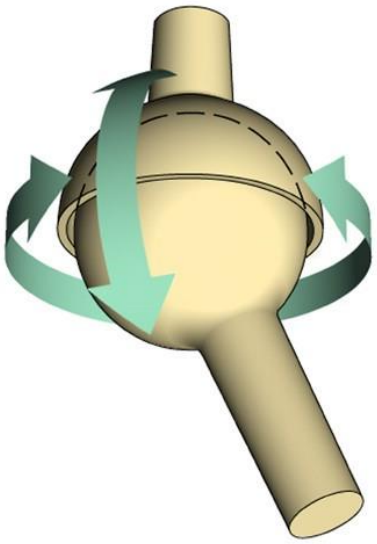

Figure 2.4 Ball and socket model [9]

The hip joint offers 3 degree of freedom for rotation in 3 planes defined in medial/lateral, anterior/posterior and superior/inferior directions of body [2]. The movements classified with these planes are defined in next section. The full functionality of ball and socket rotation is hindered by the presence of muscles like Gluteus Maximum , Hamstrings, Abductor muscles supporting the limb [3][11]. The hip joint is multi axial and the Illiofemoral, Pubofemoral and Ischiofemoral ligaments connect the parts of pelvis to femur and limit the motion along with providing stability to the joint.

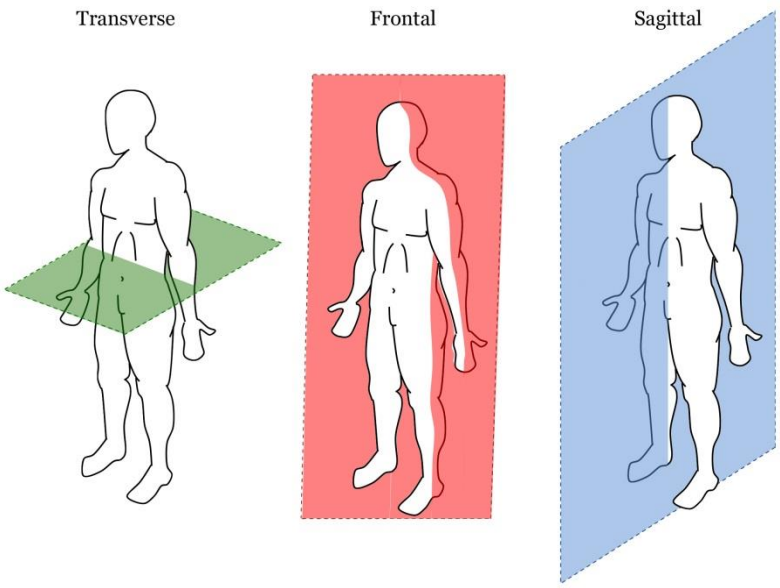

Figure 2.5 Planes of hip movement: Transverse, Frontal and Sagittal [53]

2.2 Hip Joint Center and Range of Movement

Hip joint center is the center of rotation of the ball and socket joint described above. The center acts as a point between the hip bones where the hip moments apply in order to provide a range of movement (ROM) namely; Flexion/Extension in sagittal plane, Abduction/Adduction in frontal plane and Internal/External rotation in transverse plane [11]. This ROM could be restricted due to either some pathology at the joint or due to degeneration of joint due to aging. The human motion analysis in such cases needs special attention for accurate calculation of the hip joint kinematics and kinetics [57][54].

One of the growing reasons of concern for the restriction of hip mobility is an abnormality known as Femoroacetabular impingement. Femoroacetabular Impingement (FAI) is caused by repetitive motion of hip which leads to damaging of the soft tissues as well as an abrupt growth of bone [54][59]. Due to FAI there is an abnormal collision

between the femur and acetabulum even during normal activity involving hip joint such as walking or sitting. As a result there is an uneven stress on the joints as well as soft tissues adjacent to them namely cartilage and labrum [59]. The function of these soft tissues is to distribute stress on the joint evenly and provide a cushion to the bones. Due to this stress the cartilage and/or labrum gets a tear [56][54]. The resulting degeneration, tearing of the labrum and damage to the adjacent acetabulum cartilage can lead to the development of Osteoarthritis (OA) [55]. It has been reported that this abnormality was very commonly reported in young adults who practice extreme range of motion during athletic activities [64].

There are majorly two types of FAI classified by the type of bone which causes destruction of the joint. Two affected bones of hip joint are femur and acetabulum. The abnormality associated with femur is called Cam type FAI and Pincer impingement is another variation of FAI which affects the acetabulum [56][57]. In cam FAI, an abnormal bony bump forms at the femoral head-neck junction resulting in an altered shape of the femoral head. It is mostly formed on the antereo-superior region of the head neck junction. This overgrowth of bone blocks the normal motion and rubs against acetabulum cartilage in a manner which leads to abrasion. The second type or Pincer FAI occurs due to over coverage provided by acetabular rim. Pincer FAI affects the labrum as it gets crushed between the rim of abnormal acetabulum and the femoral neck in normal movements. This may lead to deepening of the acetabulum which further increases the over coverage. Subsequently the shear forces cause damage to the cartilage in long run leading to degenerative pain.

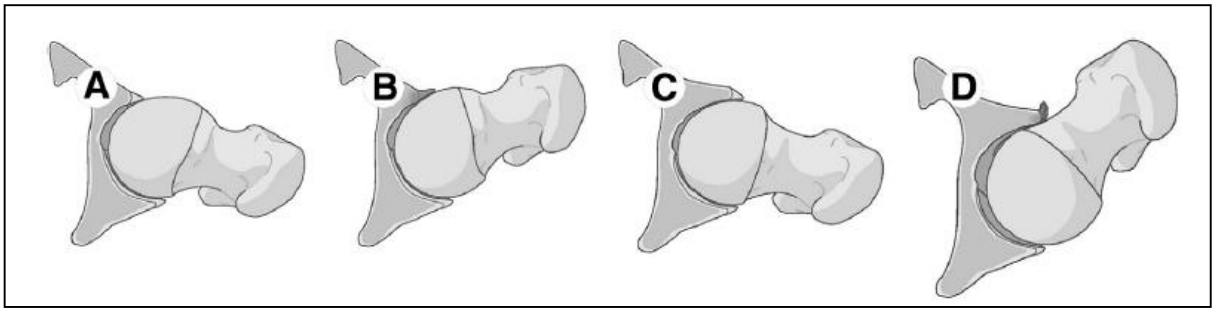

Figure 2.6 a) Cam FAI: Decreased offset at the femoral head/neck junction. b) Range of Motion (ROM) causes shear forces and cartilage damage c) Pincer FAI: Acetabular over coverage. d) Crushed labrum due to ROM by Leunig et al. [64]

The Cam type abnormality is common and is identified by alpha angle which is formed by a line drawn from the center of the femoral head through the center of the femoral neck, and a line from the center of the femoral head to the femoral head/neck junction. If the angle is greater than 55 degrees, the condition is confirmed as FAI [59].

The diagnosis of FAI consists of preliminary physical examination along with a radiographic study of hip. The X-Ray radiographs are capable of showing the bone deformation but the soft tissue damage is not visible. The onset of pain is thought to have occurred from labrum or cartilage tear [58]. Hence, MRI study is performed for examination of anatomical condition of these soft tissues.

Imaging modalities in use for detection and management of FAI:

Radiography X-Ray

Meyer et al. [63] compared radiographic projections from different views to assess the geometry of femoral head neck junction. They found that the best way to see if the hip joint was spherical or not was through Dunn view or cross table projection in internal rotation. Dunn view is the X-Ray of hip in Antereo-posterior neutral rotation, 45° of flexion and 20° of abduction [59]. The radiographic measurements include femur head neck offset, alpha angle and anterior offset measurement. These findings did not correlate with the pain and hence the soft tissues were to be considered as follows.

Magnetic resonance arthrography (MRA)

Magnetic resonance imaging allows viewing the soft tissues in body due to presence of water in them which is the principal behind MRI. To view damage in cartilage and labrum a dye is inserted to get the exact location of tear [55]. The MRA in FAI diagnosis shows the position of labrum tear as well as calculation of alpha angle can be done. So it supplements the radiographic study with additional information on soft tissue damage as seen in figure 2.7.

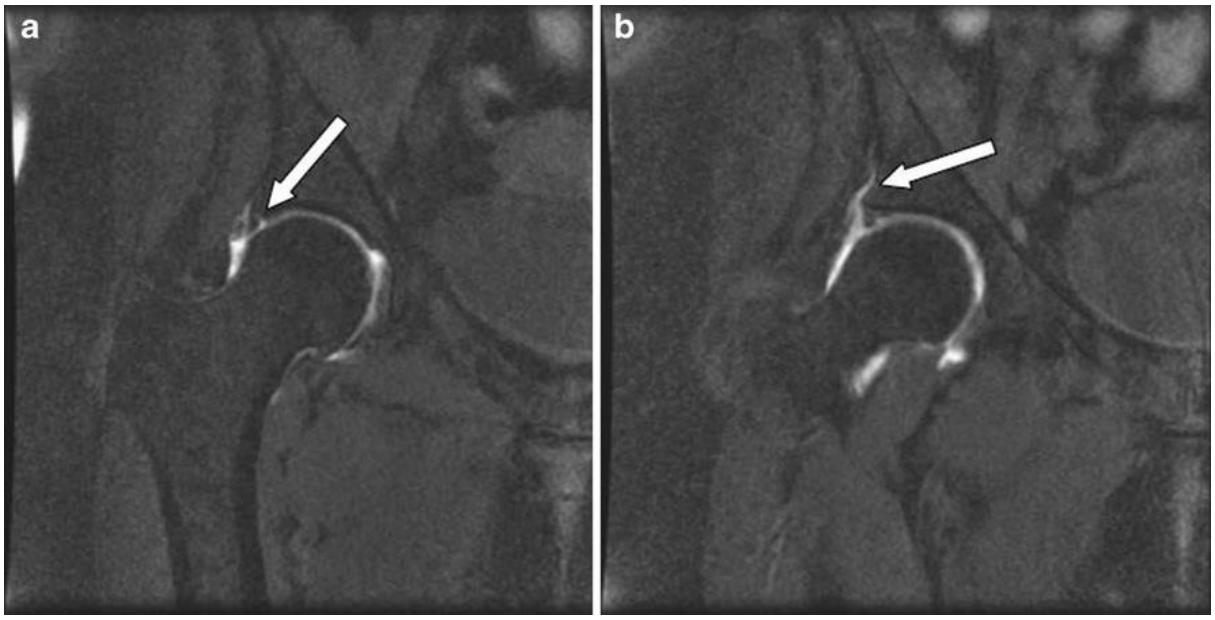

Figure 2.7 MRA of femur in FAI a) and b) showing progressive extrusion of radio opaque dye (arrow) at the site of labral tear by Banerjee et al. [59]

Two treatment options are available for treatment of FAI:

Non-Surgical management

There is no medication cure for FAI. Initial non-operative management includes lifestyle changes like avoiding excessive hip movement and regular non-steroidal anti-inflammatory agents can provide symptomatic relief. Athletes and sportsmen are advised to quit from the profession, although it is unacceptable to young professionals [59].

Surgery

For treatment of the Cam FAI, bumpectomy is suggested where the overgrowth of bone is removed with surgery [54][64]. The surgery performed can be open or arthroscopic [59]. But there is a possibility of a situation where the surgery leaves the patient with either too much removal which leads to bone fracture or too little removal which needs a re-surgery. Any labral tear should be treated with resection or repair as appropriate. This involves concerns

of serious blood loss along with damage to sciatic nerve which happens in 2% of individuals undergoing hip arthroplasty [60].

Gait analysis studies provide details on how this abnormality affects the biomechanics of normal motion. It was found that the FAI patients could not squat as low as the controls did in the study [57]. An accurate hip joint center location is required as a reference point for the gait analysis or hip moment calculation done using functional approach through human motion analysis. This center should be accurate enough to avoid errors in kinematic calculations and hence the topic has been reviewed in the coming sections.

2.3.1. Need for an Accurate Hip Joint Center

The need to find an accurate hip joint center arises from the fact that the center is desirable for accurate simulation of hip joint movements in various applications. The center of rotation has been identified as a prerequisite in surgical field for placement of hip prosthetics [11]. The accurate center of rotation is needed for better placement of the knee joint prosthetic alignment [49][50] as the axis of rotation is determined though this center. An error up to *2 mm* in determination of this axis leads to a knee prosthetic alignment error of 0.3^{o} [43]. In gait analysis applications, the bone pose is reconstructed through markers placed on skin [13][21] and there is a need for accurate hip joint center to calculate the joint angle and range of motion for rehabilitation purposes [13]. It is also used as a landmark for navigation in surgeries [25]. The errors in calculation of HJC propagate towards determination of kinematics and kinetics of the joint motion. Hence it is essential for the HJC calculation methods to give precise results [12].

2.3.2. Methods to find Hip Joint Center

Various methods have been proposed to locate HJC to calculate kinematics and kinetics of hip joint. Three main categories of methods are defined below.

Statistical modeling based method

Methods based on predictive modeling use regression equations based on morphology of the hip, such as distance between anatomical landmarks like Anterior superior iliac spine (ASIS) and Posterior superior iliac spine (PSIS). One of the studies compared by Bell et al. [14] reported HJC as a percentage of distance from ASIS in medial, distal and posterior direction. Although 95% of the times these equations based on generalized population anatomy gave the result within *27 mm* of true HJC, the question in concern was whether this accuracy would be enough for medical applications. A more recent study also reported the accuracy of such methods to be within *25-30 mm* of true hip joint center [16] . This method relies on identification of accurate anatomical landmarks which might vary depending on the expertise of the identifier [12]. Hence the result might vary from one clinician to the other depending on understanding of the landmarks.

Geometric shape based method

Hip joint center has also been estimated by using CT Scans [11], MRI [12] and X-Ray radiographs [15] of the patients. The medical imaging gives an accurate position of femur head. With the assumption that center of rotation coincides with the geometrical center of femur head, calculations are made to either fit a circle in 2D or sphere in 3D onto the surface of femur head or to use collision detection between simulated femur and acetabulum to locate the center [12]. This methodology is most accurate (within *0.1 mm* [12]) and is

considered to be a gold standard for comparison with other techniques of HJC location. Although due to the non-feasibility of sophisticated medical imaging modalities in gait laboratories and/or operation rooms there is a need for a more economical yet accurate method for identification of HJC for the purpose of gait analysis and surgical navigation systems.

Hip motion based method

Another well-known methodology to calculate HJC is through 3 dimensional stereophotogrametry [16] in which femur is rotated relative to the pelvis in order to calculate the point about which the rotations occur. This method analyses trajectories made by markers placed on body while specific movements are performed which are recorded by a motion capture system. The accuracy of such a method depends on range of motion, placement of markers, body type of patient and type and number of cycles of movement made. This method was found to pose an error of *15 mm* in a study on humans with normal ROM [30] which increases to *26 mm* [17] with a limited range of motion of hip. This method has gained popularity due to ease of calculation, accuracy and non-invasiveness [19]. This is the main topic of research here and hence is discussed in detail in further sections.

2.3 Functional Method for Hip Joint Center Calculation

Functional method for hip joint center calculation is defined as a technique to analyze the movement of femur relative to pelvic frame of reference defined by various anatomical landmarks [16]. For this approach, trajectory of movement of femur with respect to pelvis is obtained in three dimensional space. A sufficient number of markers which can be seen by optical motion capture system such as VICON [16] are placed on pelvis and femur to define

anatomical and technical frames of reference [21]. Anatomical frame of reference is defined by palpable landmarks such as RASIS, LASIS, RPSIS and LPSIS in pelvis and LE, ME and GT in femur [17][21]. Whereas technical frame of reference is defined by markers placed on skin and could vary depending on the study [21].

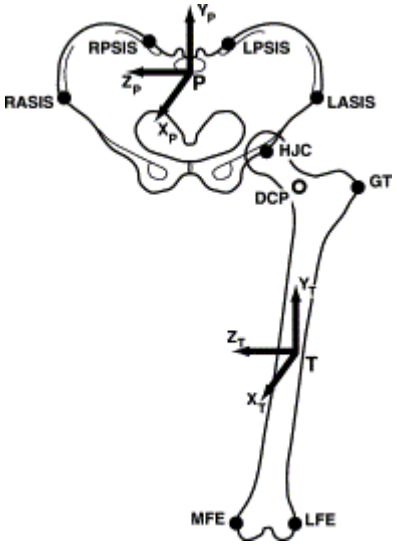

Figure 2.8 Anatomical frame of reference for femur and pelvis by Piazza et al. [17]

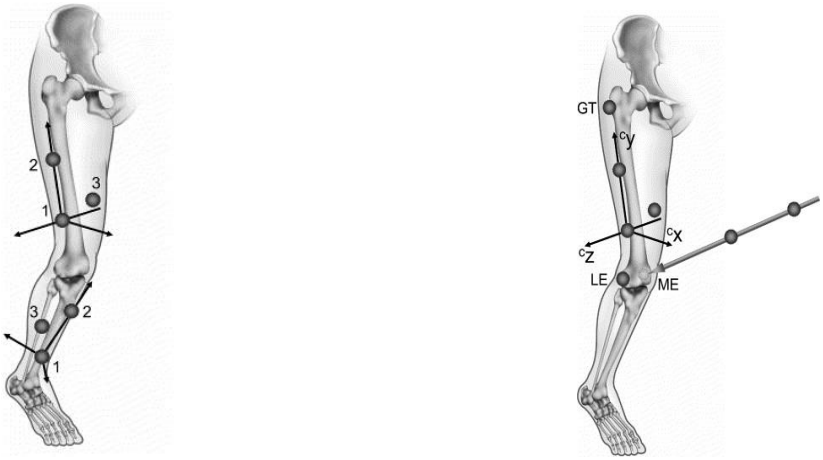

a b

Figure 2.9 a) Marker cluster on skin defining technical frame, b) Markers on bony landmarks defining anatomical frame by Cappozzo et al. [21]

External pointing device with markers placed at known distance are used for calibration of anatomical landmarks. The errors associated with the calibration process propagate to the calculation of joint kinematics and hence a precise knowledge of the palpable bony landmarks on the body is desirable.

Various studies have evaluated the accuracy of the functional method [16][17]**Error! eference source not found.**[19][20] for HJC calculation. Subsequent sections describe the major algorithms used to calculate hip joint center using the marker trajectory information obtained through various studies by means of simulation, mechanical linkages or humans.

2.3.1. Algorithms: Sphere Fitting and Coordinates Transformation

Sphere fitting

As described in earlier sections, the hip joint center is modeled as a ball and socket joint for biomechanical kinematic studies. Hence to find the hip joint center, one of the approach taken by various studies [13][16][19][20] is to model the joint as a sphere to be centered at the HJC. Once the marker trajectories of femur with respect to a fixed coordinate system (pelvis) are known over a period of time, these trajectories are modeled to trace a sphere and the center is calculated using geometric sphere fitting equations. Most common approach is to initialize a sphere with center say c_0 in global orthogonal coordinate system. If f_{ij} gives the known positions (on the moving segment, say femur) of m markers ($j = 1$ to m) in N time frames ($i = 1$ to N), then for each time frame, the Euclidean distance between the marker position and sphere is minimized [16][19]

$$\sum_{j=1}^{m}\sum_{i=1}^{N}\left(\|f_{ij}-c\|^2-r_j^2\right)^2 \quad (1)$$

c is the center calculated at each time frame for all markers iteratively until it converges to minimize the error and r is the radius of sphere calculated from marker position. This solution is also known as Quartic Sphere fit [16] and has a closed form solution. Although it was found by Halvorsen et al. [35] that the solution of *(1)* is biased and does not converge to true center. The bias gets removed when solved iteratively using a correction term.

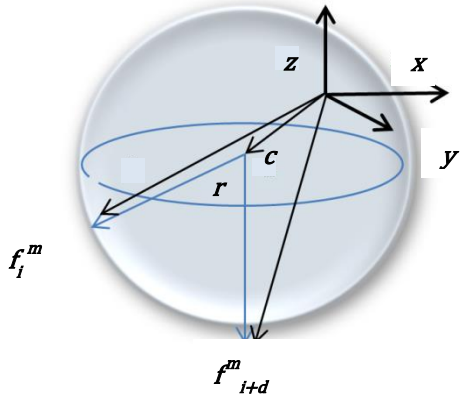

Figure 2.10 Depicting the sphere traced by marker m, at time instance i and $i+d$ with radius r and center at c. x, y and z are unit axes attached rigidly to pelvis

Coordinate transformation

Ehrig et al. [20] evaluated numerous algorithms under the two major categories namely: Sphere fitting as described above and Coordinate transformation. It was observed by the authors that sphere fit method could only be applicable in case one of the segments of hip joint is stationary and gives a constant center of rotation. Even if the pelvis is more stationary, it is not completely immobile and its associated movement is not taken into consideration in sphere fitting algorithms. Another category of algorithms namely

Coordinate Transformation was evaluated and compared to geometric sphere fit methods for the first time by Ehrig et al. [20]. In this category a local frame of reference is defined on the moving segment of body using three or more markers and a point, $\boldsymbol{c}$, is found throughout the motion which is mapped from a local frame of reference to global frame of reference satisfying the condition given in equation *(2)*.

$$\sum_{i=1}^{n} \| R_i \tilde{c} + t_i - c \|^2 \qquad (2)$$

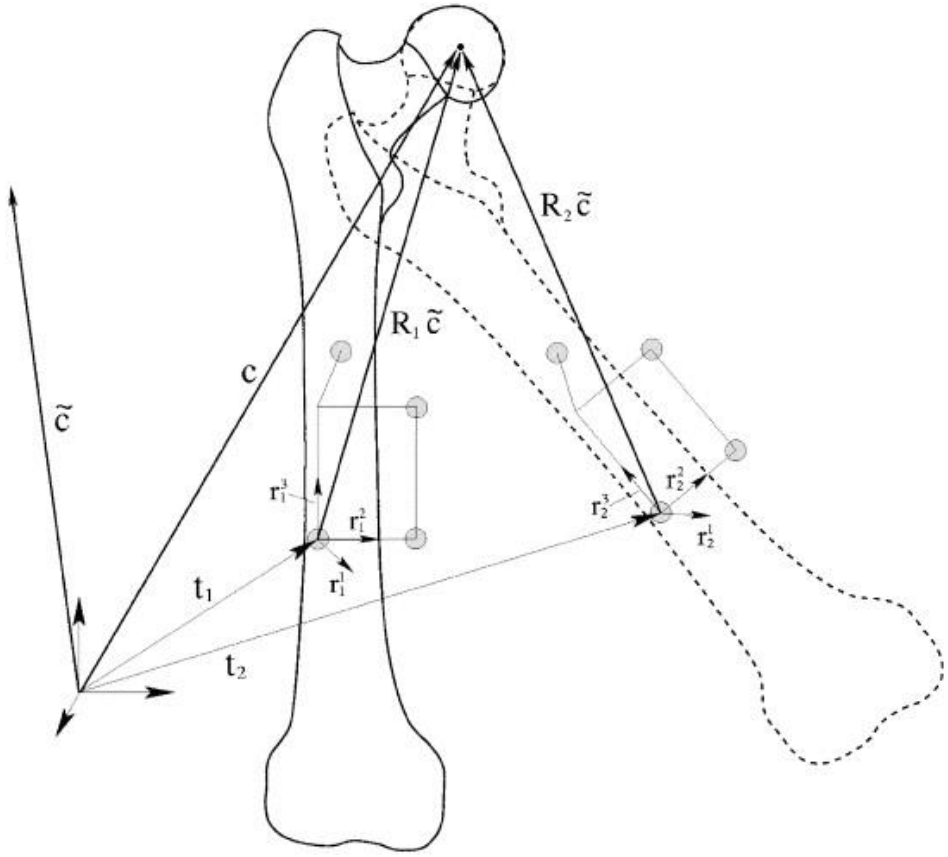

Figure 2.11 Local femoral frame of reference with orientation $\boldsymbol{R}$ and position $\boldsymbol{t}$ with respect to a global frame by Ehrig et al. [20]

The authors also devised an algorithm to accommodate the movement of pelvis rather than just the femur. This algorithm utilizes transformation of coordinates of center from local pelvic and femur frame of reference to an appropriate global frame such that a common point with least movement is determined as HJC. This is known as Symmetric Center of Rotation Estimation popularly known as SCoRE

$$\sum_{i=1}^{N} \left\| R_{fi} c_f + O_{fi} - \left(R_{pi} c_p + O_{pi} \right) \right\|^2 \qquad (3)$$

R_{fi}, R_{pi} are the orientation matrices and O_{fi}, O_{pi} are position vectors attached to femur and pelvis respectively for time frames $i = 1$ to N. Equation *(3)* is minimized to get c_p and c_f which are center of rotation in pelvic and femur local coordinate systems respectively. An estimate of accuracy of SCoRE is obtained by calculating SCoRE residual [36] which is a measure of the distance between c_p and c_f after converting into an appropriate global coordinate system. This method was applied and compared with sphere fit on various human and cadaver studies as well. While the SCoRE algorithm tested on simulation studies yields more accurate results *(0.5 cm)* than sphere fit method when both segments were in motion, the study on human by Sangeux et al. [30] and on cadaver by Lopomo et al. [28] presented sphere fit to be more accurate. Therefore, there is still a need to come up with the best algorithm and/or functional technique to be applied to human studies for more accurate results.

2.3.2. Classification of Functional Studies based on Type of Data

Mechanical linkage based studies

An attempt to propose an optimized protocol for studies on functional estimation of HJC was made by Camomilla et al. [16]. The authors studied effect of various factors such as type and amplitude of movement, algorithm used, distance between markers and location of cluster of markers on the calculation of hip joint center. Based on this study an algorithm known as bias compensated sphere fit with a movement called as "Star Arc" [16] with various flexion/extension, abduction/adduction and circumduction motion gave the most accurate result when markers were placed far from each other but close to the joint center.

The authors indicated that the errors in calculation of hip joint center through functional approach could be reduced to *1 mm* by using these optimal conditions in absence of soft tissue artifact (discussed in upcoming sections). This study was performed using mechanical linkage, which is a model resembling the human hip joint consisting of metallic rods connected through a ball and socket joint. The model is incapable of depicting real hip joint as there are no soft tissues restricting the motion. Hence the mechanical setup used to obtain the result for HJC was distant from the human based experimental conditions which report an error of up to *13 mm* [21]. Advantage of mechanical linkage based studies is that a true center of rotation is known for checking the accuracy of algorithm.

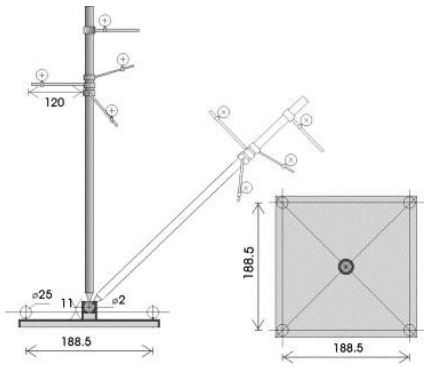

Figure 2.12 Mechanical linkage front view (left) and top view (right) used by Camomilla et al. [16]

Digital simulation based studies

Virtual markers illustrating positions of anatomical landmark on pelvis and femur were generated using computer simulation in a study [20] to test the accuracy of various algorithms being used to calculate HJC through functional approach. Utility of simulation based experiments is to generate large number of samples of data with varied variables in terms of ROM, amplitude, random noise, different cluster of markers to check the effect of these variables on a new algorithm to find HJC. Begon et al. [18] employed trajectory information from markers placed on a human participant to simulate the model to replicate human based errors and obtained accuracy within *4 mm* which was close to the ones based on mechanical linkage. This study also recommended that low amplitude movements with more repetitions produce minimum errors whereas Camomilla et al. [16] advise the use of maximum possible range of movement. Since artificial noise is added to simulate conditions similar to studies on humans, simulation based studies are useful only for testing functionality of an algorithm but does not guarantee its replication in human based studies.

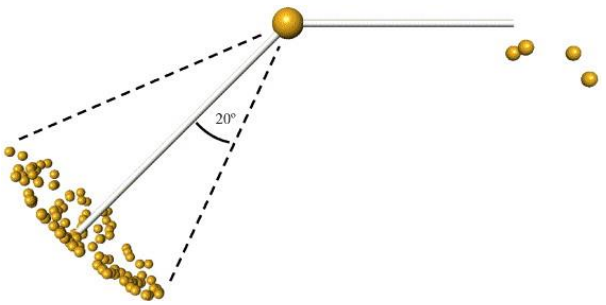

Figure 2.13 Simulation of 4 markers on pelvis and femur each and rotation of femur by *20°* by Ehrig et al. [20]

Cadaver based studies

Mechanical linkage and simulation based studies lack the information of marker deformation due to skin stretching and tissue wobbling known as Soft Tissue Artifact (STA) when markers are placed on skin [23] In vitro studies have been performed on cadavers to test the accuracy of functional algorithms [26]. These studies provide a way to measure the soft tissue artifact by various techniques and at the same time assess the accuracy of algorithm through skin markers. Markers are attached to a pin tracker that can be inserted in the bone so that true bone trajectory information is available which is considered to give the gold standard data for comparison with markers placed on skin. The functional algorithms which provided an accuracy of more than *1 mm* when tested with simulation and mechanical linkage gave an error up to *10 mm* when placed on skin. Sphere fit algorithm was more accurate with reduction in range of motion [26] whereas transformation technique was more accurate in presence of pelvic tracker to accommodate the error due to movement of both segments [28].

Human based studies

All the previous studies form a basis for testing the functionality and accuracy of algorithms to be finally used in human based studies. The need for functional HJC arises from the fact that a non-invasive motion analysis based method could give an estimate of HJC close to the actual center for various applications in surgical navigation system or gait analysis. The studies based on human participants show an accuracy of up to *13 mm* [19]. A recent study on normal human population suggested that geometric sphere fit algorithms gave an accuracy of up to *20 mm* and performed better than coordinate transformation techniques [30]. The errors increase by an order of magnitude when compared with the simulation data results [30]. Studies performed on humans need an estimate of actual hip center through imaging modalities [32] to calculate the error. Peters et al. [33] proved the utility of ultrasound as a possible tool to assess the actual HJC within *4 mm* of MRI through 3D ultrasound imaging. This was used as a validation methodology in human based experiments [29][30].The errors found in human based studies with markers placed on skin are said to come from so called soft tissue artifact which is the topic to be covered in coming sections.

Apart from the traditional way of determining the joint center through motion tracking of markers placed externally on the skin, we are aiming to improve the calculations by introduction of an imaging modality known as ultrasound imaging, as mentioned in section 1.3, to measure the change in tissue thickness while the hip is moved. In the next section we will briefly describe the characteristics of the image and how we process the image to track an edge in it.

2.4 Ultrasound Imaging and EdgeTrak

Ultrasound is an imaging modality which works on the principal of sending a sound wave in the frequency range more than 20 KHz through the body and then measure the reflected wave which would give information regarding the depth of the tissue under measurement. The modality is inexpensive apart from being portable and poses no known risk to humans. The main use of this imaging is to view morphological details of soft tissues such as fetus or heart. The system consists of a transducer which converts electrical signals to acoustic waves and transmits it to the body, while also acting as a receiver which receives the echo waves returning after reflection from body tissues. The pixels in image represent the location of the anatomical feature in the body that has reflected the signal and the brightness corresponds to the strength of the echo. Besides its various advantages, ultrasound imaging suffers from low signal to noise ration and low image resolution compared to its counter parts such as MRI or CT.

Major reasons for including ultrasound imaging in the context of improving HJC calculation through motion capture are: Real time measurement of depth of bone during hip movement, non-Invasive imaging, feasibility of integration with motion capture system and portability. We needed to track the change in the tissue thickness while hip is being flexed when simultaneously the movement of markers placed on skin is being recorded. We observed that the bone surface at thigh is visible as an edge in ultrasound image while person is standing still and even while the hip is flexed when transducers are aligned vertically to the length of the bone. Hence we needed to track the edge of the bone in the images in order to get the information on change in tissue thickness covering the bone.

2.4.1. EdgeTrak : Algorithm for Tracking Edge in Ultrasound Image

The EdgeTrak [47] is software developed by Li et al. [47] in 2004 which is used to track the surface of the tongue in ultrasound images. Ultrasound images have high speckle noise occurring due to interference of the coherent waves. Due to the presence of high contrast noise, it is not easy to track the edges in the image through traditional edge detection methods. Li et al. [47] used an active snake model along with the incorporation of a constraint of intensity homogeneity. It is able to track the surface of the tongue in a series of real time images acquired while speaking some words.

The active snake model works with a few contour points given by users on the ultrasound image, which are interpolated to get smoothly connected points through B-Spline interpolation. These points are then attracted towards the edge by minimization of internal and external energies. The internal energy governs the smoothness of the curve and makes sure to track the edges even in discontinuities. While the external energy consists of the intensity gradient change along with a local region based intensity information. This component connects the contour points to the image. The intensity homogeneity constraint avoids tracking the speckle noise which also has high intensity gradient.

A prime reason for using EdgeTrak is to ensure an automatic edge tracking system which can track the edge of an object through a sequence of images while the position and shape of the edge is being deformed. Also, using existing algorithms for edge detection cannot distinguish between similar intensity edges presented by the dense muscle overlaying the bone at the front of thigh. Since in EdgeTrak, we initialize the first frame near the edge of

interest, the muscle tracking is avoided and sequence of images are tracked through dynamic programming by taking the contours of previous frame as the initialization.

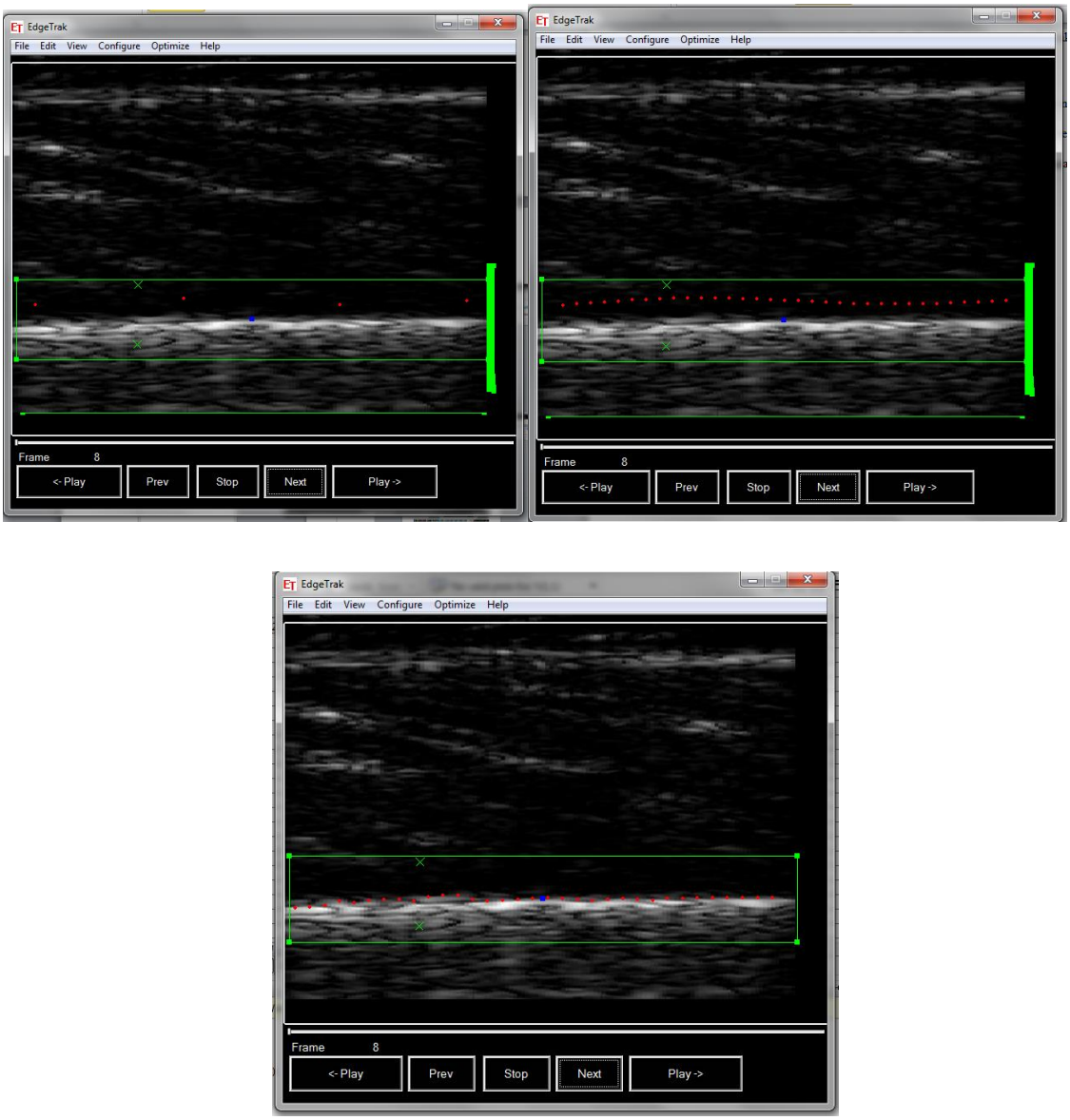

Figure 2.14 EdgeTrak [47] showing a) Contour point initialization b) B-Spline interpolation of points into a smooth curve c) The optimized tracking of edge of interest in spite of other high contrast features.

Based on the reviewed literature in previous section, we present the overview of methodology used in this research work for calculating the hip joint center in human based studies using functional method and further improving the same for more accurate results in the upcoming section.

Chapter 3. Overview of Methodology

3.1 Objective

The objective of this research is to use ultrasound as an adhoc modality with human motion analysis experiments in order to decrease the error in finding hip joint center using existing algorithms based on coordinate transformation methods. The coordinate transformation algorithm (SCoRE) mentioned in section 2.3.1 will be used to calculate the hip joint center using the trajectories made by markers on thigh and pelvis , placed on skin. This is explained further in the section below. We will make an attempt to measure the change in the distance between skin and bone (femur) during leg movement in a non-invasive manner using ultrasound imaging modality. This information will be further used to recalculate the position of markers placed on thigh in a global frame of reference and the new marker positions will be used to recalculate the hip joint center.

3.2 Calculation of Hip Joint Center

We need orientation matrix and position vector attached to the pelvis and thigh in order to calculate the joint center of rotation using SCoRE algorithm. Using three marker positions on each segment, say m_1, m_2 and m_3, the joint positions can be defined as a position vector of any of the markers for all time frames recorded. To calculate the orientation/ rotation

matrix we use two methods: Unit vector and Singular Value Decomposition.

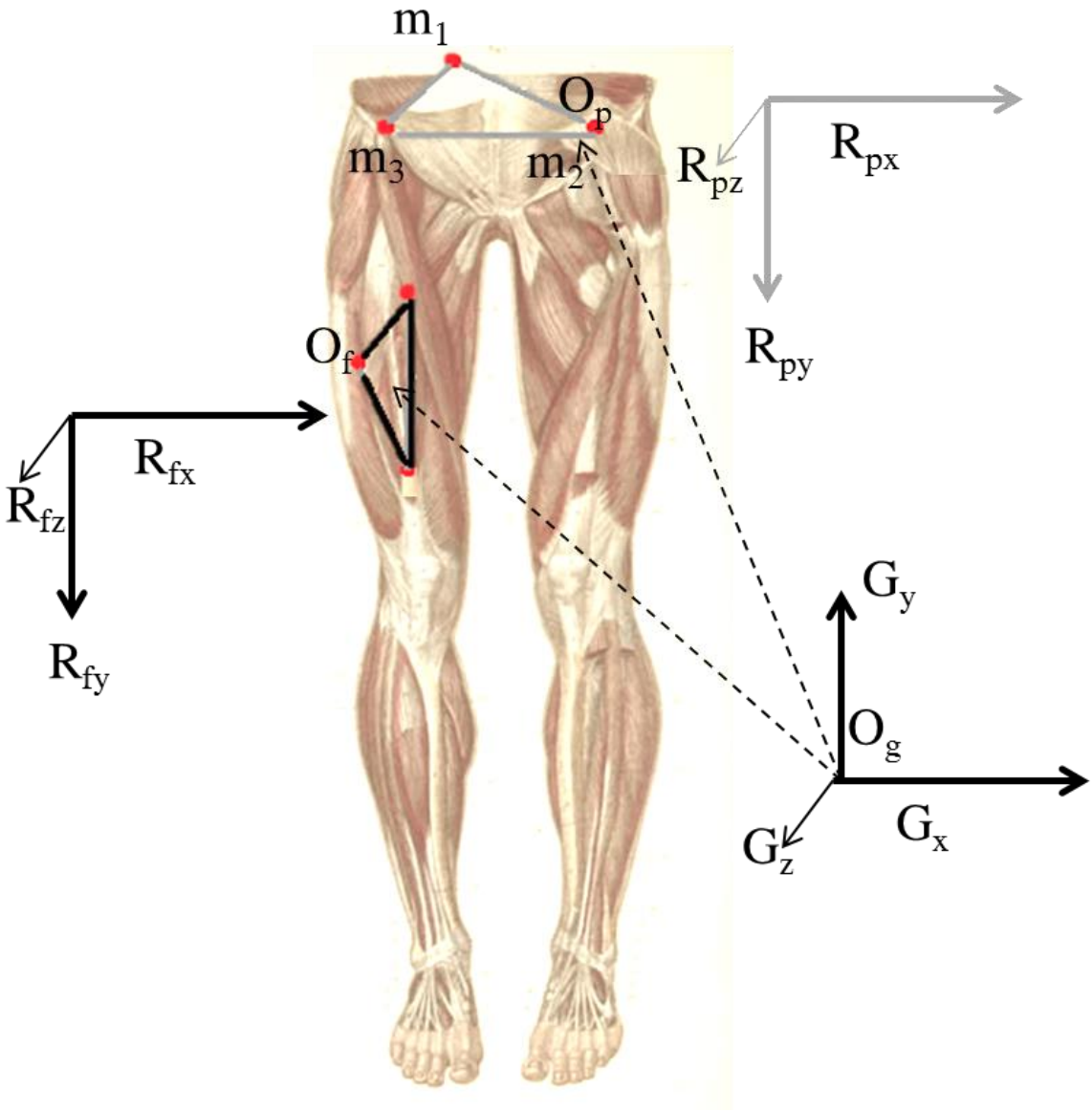

Figure 3.1 Representation of skin marker clusters on thigh and pelvis forming the local frame of references ***Rf,Of*** and ***Rp,Op*** respectively with respect to global frame of reference ***G,Og*** (Human thigh image obtained from Anatomy Atlas [4])

3.2.1. Calculation of Rotation Matrix

Using the marker positions on each segment, the orientation / rotation matrix can be calculate as follows

$$X = |m_2 - m_1|/norm(m_2 - m_1) \quad (4)$$

$$Z = crossProduct(|m_3 - m_1|/norm(m_3 - m_1), X) \quad (5)$$

$$Y = crossProduct(Z, X) \quad (6)$$

Where $/m_2 - m_1/$ is the vector distance between two markers for N time frames and $norm\ (m_2 - m_1)$ is the magnitude of the distance between markers for all frames. $crossProduct\ (A,B)$ gives the vector cross product between two vectors A and B. Thus X, Y and Z are orthonormal unit vectors and $R = [X\ Y\ Z]$ is the rotation matrix of a segment with respect to a global frame of reference G. Hence we get the rotation matrices R_f and R_p corresponding to the segments femur and pelvis respectively.

Another way to calculate this matrix is by using Singular Value Decomposition (SVD) algorithm proposed by Soderkvist and Wedin [48]. In this algorithm, the position of all markers for all the frames, in a cluster attached to a segment is registered onto the position of a static pose *i.e.* the first frame of the cluster. Here we explain this algorithm for calculation of pelvic rotation matrix R_p,

Let's say for markers m_1, m_2 and m_3 attached to pelvis, we have two positions in time recorded at 1st frame and Nth frame. Let the positions be x_1, x_2, x_3 for frame 1 and y_1, y_2, y_3

for frame N. Then two matrices are constructed using the positions of markers in two frames such that

$$A = [x_1 - mean(x), x_2 - mean(x), x_3 - mean(x)] \quad (7)$$

$$B = [y_1 - mean(y), y_2 - mean(y), y_3 - mean(y)] \quad (8)$$

Where $\boldsymbol{mean(x)} = \frac{1}{n}\sum_{i=1}^{n} \boldsymbol{x}\,(\boldsymbol{i})$ and $\boldsymbol{mean(y)} = \frac{1}{n}\sum_{i=1}^{n} \boldsymbol{y}\,(\boldsymbol{i})$ are the average of positions of all markers in frame one and any frame N resp. And the rotation matrix is determined by getting the minimum of the function

$$min\left|\left|RA - B\right|\right|_F \quad (9)$$

Where $\left|\left|Z\right|\right|_F = \sum_{i,j} z_{i_j}^2$ and equation *(9)* is solved using the SVD as follows

$$C = BA' \quad (10)$$

$$[P, Q, T] = svd(C) \quad (11)$$

$$R_p = P(diag[1\ 1 \det(PT')])T' \quad (12)$$

$$O_p = mean(y) - R(mean(x)) \quad (13)$$

Where equation *(11)* is solved using the *svd* function in MATLAB for singular value decomposition of a matrix into orthonormal components $\boldsymbol{P, T}$ and a diagonal matrix $\boldsymbol{Q}$.$\boldsymbol{X'}$ *is* the transpose of any matrix $\boldsymbol{X}$. These rotation matrices are calculated from markers attached on the segments, namely femur, pelvis and probe. Based on the calculation of rotation matrix and position vectors defining local frame of references, further algorithm can be discussed.

3.2.2. Coordinate Transformation Algorithm

Using the rotation matrices calculated by the methods explained in section 3.2.1, the coordinate transformation algorithm from Ehrig et al. [20] is presented as follows,

$$\begin{bmatrix} R_{f_1} - R_{p_1} \\ . \\ . \\ R_{f_N} - R_{p_N} \end{bmatrix} \begin{bmatrix} C_f \\ C_p \end{bmatrix} = \begin{bmatrix} O_{p_1} - O_{f_1} \\ . \\ . \\ O_{p_N} - O_{f_N} \end{bmatrix} \quad (14)$$

Where R_{fi} and R_{pi} are the rotation matrices associated with femur and pelvis resp. for frames $i = 1 \text{ to } N$ and O_{fi} and O_{pi} are the corresponding translation vectors calculated from the mean of marker positions in local frame of reference indicating the origin of the segment as shown in equation (13).

These over determinate system of equations are solved using MATLAB backslash operator '\' to get a least square estimation of centers in local femur and pelvic frame of reference; C_f and C_p respectively.

3.2.3. Evaluation of Algorithm Accuracy

The calculated centers in local frame of reference of femur and pelvis should ideally coincide as the center of rotation of the whole joint is one point common to both the segments. Hence the inaccuracy in the algorithm is reported as the distance between the two calculated centers C_f and C_p.

$$r = |C_p - C_f| \quad (15)$$

Where r is the "SCoRE residual" which is proportional to the error compared to the actual hip joint center in the condition where it is a known quantity.

Ehrig et al. [36] validated through a statistical model that, the residual is proportional to the actual error estimated using a known hip joint center. They coined the term "SCoRE residual" which is equal to the Euclidean distance between C_f and C_p after transforming into a common frame of reference. Hence, by using this relation a decrease SCoRE residual will indicate an increase in accuracy of the algorithm. We use this measure to estimate the

accuracy of algorithm and also to compare the results obtained amongst different participants. We follow its proportionality proved by Ehrig et al. [36] with error compared to the actual HJC and provide a measure of the accuracy of algorithm in case the actual center is not known.

3.3 Complications

The accurate estimation of joint center of rotation depends on how precisely the rotation matrices depict the orientation and the position vectors represent the position of the segment pose. This would depend on the position of markers. If the markers were rigidly attached on the bone, the $\boldsymbol{R}$ and $\boldsymbol{O}$ would perfectly represent the segment and hence result in accurate center determination.

The calculation of hip joint center through human motion analysis experiments suffers from error due to movement of markers placed on skin rather than directly on bone. This is known as soft tissue artifact (STA). Due to this artifact, there is an error in reconstruction of bone from markers placed on skin.

3.3.1. Soft Tissue Artifact

Functional algorithms have been demonstrated to be accurate enough to find HJC using non-invasive motion capture system. Although great accuracy was found in simulation studies, the errors increased by more than *10* times in human based experiments. Leardini et al. [23] have prepared a thorough analysis of a common source of error in human based motion analysis which is said to be caused by movement of skin markers relative to the underlying bone. Due to this error, the measurements made with the position reconstructed through skin markers would not represent a true bone. STA is quantified as the amount of

displacement of markers on skin relative to underlying bone fixed frame of reference. This has been studied through invasive measures where pins are inserted in bone with markers on them defining the bone reference system along with markers on skin [26][27][28]. Some studies have used external fixation devices to get a bone fixed frame of reference [38][39]. Alexander et al. [38] quantified the limb segment pose estimation error through the analysis of change in limb shape by tracking underlying bone trajectory for a particular task and corrected the position and orientation by *33%* and *25%* respectively. Whereas Ryu et al. [39] modeled and compensated the displacement of anatomical landmarks through skin movement analysis by *40-80%*. While interval deformation technique defined in former study mandated a previous knowledge of marker trajectory with respect to bone, the latter one required precise anatomical landmark identification which varied with expertise. Due to invasive nature of these studies, a common consensus for soft tissue artifact compensation is still a topic of research. In a partially non-invasive study which combined X-Ray fluoroscopy to measure the STA, it was found that while the STA could be generalized for a specific motion type, it varies with subject and location of markers.

3.3.2. Minimization of Error in Optical Motion Analysis

A comprehensive study on methods to minimize STA errors has been presented by Leardini et al. [23]. Methodologies range from solidification procedure, where three markers on skin are chosen to form a triangle with least deformation over a period of time, to anatomical landmark calibration where in the markers placed on bony landmarks such as greater trochanter and medial/lateral epicondyle are tracked over time to compensate for skin displacement through least square minimization approach. Minimization of functional HJC error due to STA based on statistical shape analysis methods have been suggested recently

[41]. However these methods overcome the problem of distortion of the shape of the clusters over time, the issue of its non-association with underlying bone still remains unsolved. These studies have only provided a measure to tackle the error with associated algorithm (SCoRE) [20], whereas in human based experiments [33] it was proved that geometric sphere fit provide a better estimate of HJC. Hence there is a need to eliminate the issue of STA in functional HJC independent of algorithms to be used.

3.3.3. Algorithm for Soft Tissue Artifact Compensation

It was observed that amongst other STA compensation algorithms, Alexander et al. [38] advised a technique that not only takes into consideration minimization of displacement of markers on skin, but also incorporates the trajectory information of markers moving with respect to underlying bone.

The algorithm requires knowledge of marker trajectory which was found to be Gaussian for the task of stepping up a stair. This trajectory along with a Gaussian noise gives an estimate of the pose of underlying bone and accommodates any change in limb shape due to STA over time. If a cluster of m markers with position $F(i)$ (in global frame) in $i = 1$ to N time instances is given with respect to its center of mass (C) and rotation matrix constructed from inertia Eigen vectors (E), then markers position in local cluster frame is given by

$$L(i) = E(i)^{-1} (F(i) - C(i)) \quad (16)$$

If bone pose is known with an Orientation $B(i)$ and position $O(i)$, then the skin markers with respect to the bone embedded system can be represented as

$$R(i) = B(i)^{-1} (F(i) - O(i)) \quad (17)$$

This solution is indeterminate since B and O are unknown and cannot be known unless invasive measures are taken to get this pose estimation. R and L are said to be coincident when the subject is in static position and they could be estimated using rigid body transformation from each other.

An estimate of R is made through a knowledge of trajectory of markers $d(a_i)$ with respect to bone and an additional noise $v(i)$. Through this, L could be estimated and minimized with chi square test to get the parameters for trajectory $d(a_i)$, where d is the trajectory defined with parameters a over i time instances.

With this parameter identification, transformation between marker cluster to bone cluster can be obtained using inertia tensor Eigen value decomposition at each time step [38]. This model generates bone pose X, Y and Z coordinates which were compared to the bone pose estimated by markers placed on an external fixation device. The interval deformation techniques used in this study has shown to improve the estimation of bone pose from skin markers rather than rigid body assumption by *29%*.

3.4 Solution Overview

Based on the algorithm described in section 3.3.3 we came up with the idea of tracking the bone movement with respect to skin which could be used to get the trajectory of marker with respect to bone as needed in the previous algorithm for registration of skin based frame of reference to bone fixed frame of reference.

Ultrasound is an imaging modality which is considered non-invasive when compared to other imaging modalities such as X-Ray radiography. This is a modality in which bone is visible as a dense white tissue compared to the other soft tissue due to its highly dense

nature. We have attempted to use the ultrasound imaging to track the position of bone (femur) in the moving segment while integrating it with motion capture system to simultaneously track the movement of skin markers. By placing markers on an attachment to probe we can get an estimate of 3D position of the image plane in a global frame of reference. Also, a rigid attachment on probe with markers on it would act as a probe fixed frame of reference which moves rigidly with the thigh and also gives value depth of bone at the same time. This information will be used to translate the skin marker position on thigh to match the trajectory of bone by making transformations of markers in probe's frame of reference.

After getting a new position of the skin markers on thigh in global frame of reference, the rotation matrix and position vector (New_R_f *and* New_O_f) will be recalculated for thigh based on equations to calculate rotation matrix explained in section 3.2.1 and then used to solve equation *(14)* to obtain new center of rotation and consequently SCoRE residual will be measured and compared. We expect the SCoRE residual to decrease when New_R_f *and* New_O_f are used for solving for the centers and hence claiming to have improved estimate of bone position based on bone depth information during hip movement from ultrasound imaging.

Chapter 4. Experimental Procedure and Data Aquisition

The experimental setup consisted of ultrasound imaging machine (Picus, Esaote Europe) and linear probe (L10-5, *5 MHz* operating frequency, width *4 cm*). The motion capture system consisted of *6* VICON MX40 cameras operating at the frame rate of *120 Hz*. *9* retro reflective markers were used, *3* each on thigh and back, and *3* on probe with an extension to track the position of probe movement. Four researchers took part in the initial exploratory research needed to form the design of the research after signing an informed consent with an ethics approval from Carleton University. The ultrasound images were obtained at a frame rate of *30 Hz* for *6* seconds which gave *180* frames of recording for each capture.

For initial exploratory research, *16 (4*2*2)* recordings were measured for each participant with motion capture and ultrasound being recorded simultaneously. Four movement types namely: Flexion with knee bent (KB), Flexion with knee straight (KS), Abduction, and Circumduction were performed so that ultrasound transducers were placed in two positions: vertically and horizontally aligned to the underlying bone on thigh. Probe was also placed at two positions on thigh, at front and on side (laterally). For each movement initially the participant stood still. After a count of three, ultrasound recording was initiated with a slight push given to ultrasound probe perpendicular to the skin surface for synchronization with the VICON's recording of the position of markers after which the hip movements were made one at a time and the VICON recording was on before and after the ultrasound recording.

a)

b) c)

Figure 4.1 Experimental Setup showing a) VICON MX40 *6* cameras with participant in stationary pose b) ultrasound machine c) ultrasound probe with attachment for markers

The Workflow of Experimental Procedure

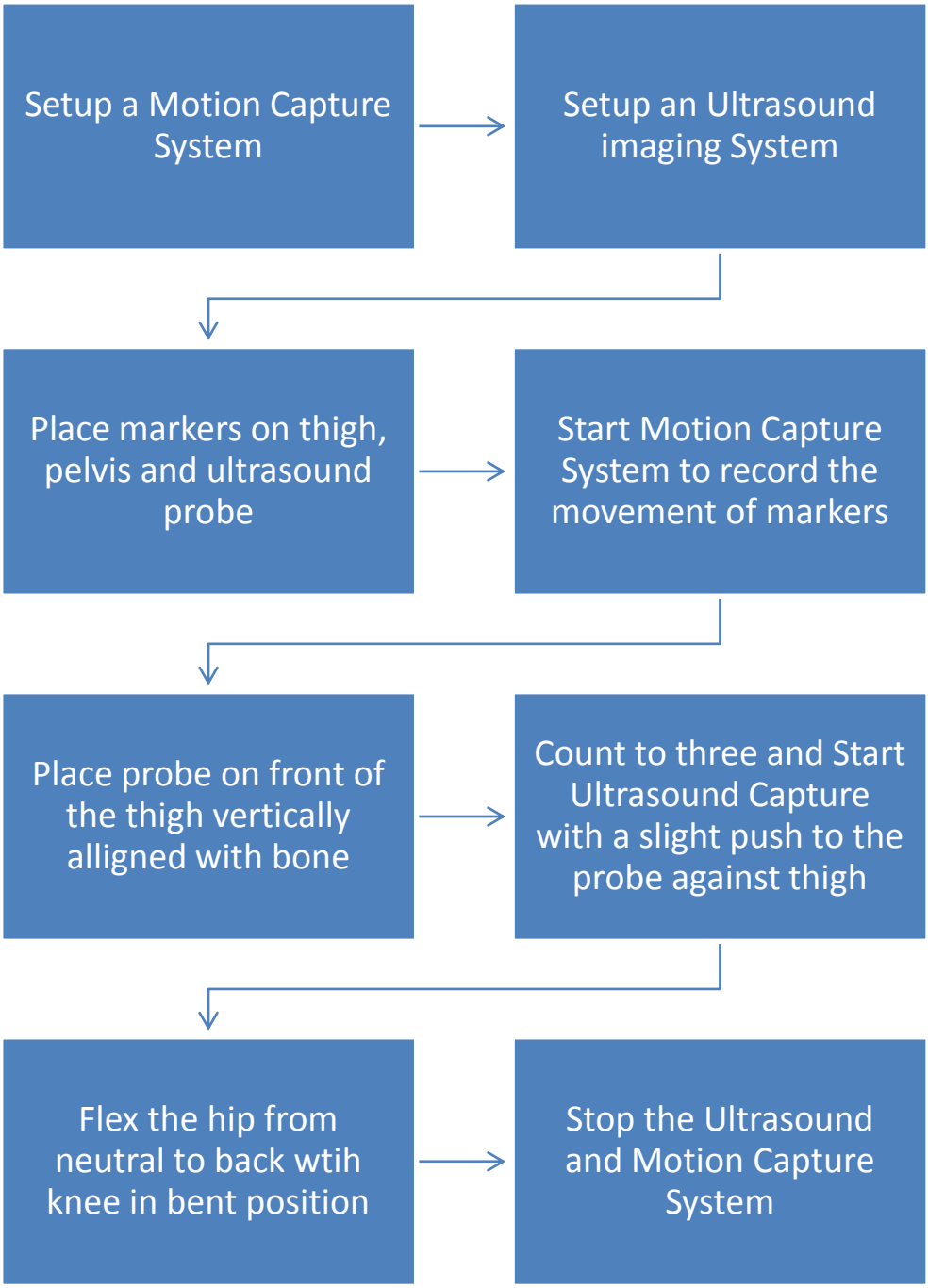

The ultrasound images were processed using MATLAB. The bone was detected as a straight line when transducer was aligned vertically to the bone as opposed to a curve when it was aligned horizontally as shown in figure 4.2.

The software EdgeTrak [47] was used to track the position of bone in ultrasound images. The images with transducer in horizontal alignment, figure 4.2 d, were noisy with a lot of frames missing the bone information due to possible slipping of the probe, hence only vertically aligned images were processed. Contour points were initialized for one frame and automatic edge detection was performed using EdgeTrak [47]. The contour points were exported as *100* x and y coordinates for *180* frames and processed with MATLAB. The average y coordinate of the contour points gave the tissue thickness information for *180* frames over *6* seconds.

When participant was at rest, the bone was considered to be in a neutral position. The thickness obtained by the first frame of ultrasound gave this information. Using MATLAB, the displacement of bone from its neutral position with respect to skin was obtained to calculate the change in tissue thickness for each subsequent ultrasound frame. The initial push given to the probe in order to synchronize the ultrasound frames with VICON motion capture data is seen as a glitch in the image, figure 4.3, due to a sudden decrease in tissue thickness before movement occurs. This is used to identify the start of the motion in ultrasound images and synchronized with VICON based on time stamping.

Table 4.1 Displacement of skin marker on thigh in 3D (VICON) and bone (femur) in 2D (Ultrasound) with motion type "Flexion (Knee Bent)"

Participant	**Probe location (On thigh)**	**Maximum Marker (thigh) Movement in space (cm)**	**Maximum Bone (thigh) Movement wrt skin (cm)**	**Average Bone (thigh) Movement wrt skin (cm)**
1.	Front	31.55	1.486	0.94
	Side	37.03	0.705	0.32
2.	Front	28.61	0.476	0.216
	Side	21.52	0.038	-0.020
3.	Front	26.69	0.779	0.608
	Side	26.89	0.731	0.370
4.	Front	30.11	0.866	0.486
	Side	17.55	0.414	0.161

Table 4.2 Correlation of synchronized data for movement of marker on skin (VICON) and bone (Ultrasound)

Participant	**Probe location (On thigh)**	**Correlation coefficient (r) (P<0.001)**
1	Front	0.869
	Side	0.861
2	Front	0.527
	Side	-0.251
3	Front	0.612
	Side	0.748
4	Front	0.581
	Side	0.511

The displacement of skin markers was calculated as the absolute difference of average marker's position on thigh between two consecutive frames. This gave a qualitative idea on the movement of thigh in space. In Table 4.1, the maximum displacement of the skin markers in a global laboratory frame of reference is reported along with the maximum and average displacement of bone from its neutral pose with respect to skin obtained from ultrasound for four participants.

A correlation was obtained between displacement of markers on skin in space and the movement of bone from its neutral position after synchronization of VICON and ultrasound frames such that for every four samples of VICON data there was one ultrasound data point.

Compared to others, one participant exhibited maximum displacement of bone in flexed position from its neutral pose when at rest. As seen in Table 4.2, the correlation between displacement of markers on skin and the displacement of bone from its neutral position was maximum for participant 1. Hence, for the purpose of qualitative analysis, participant 1's data is analyzed in the thesis to establish the algorithm for defining a bone fixed frame of reference based on the bone depth information from ultrasound for Flexion (KB) with probe placed at the front of the thigh. Subsequently, time frames giving maximum correlation for other participants are identified and the algorithm based on participant 1's data analysis is applied to compare the results of hip joint center calculation using the coordinate transformation algorithm.

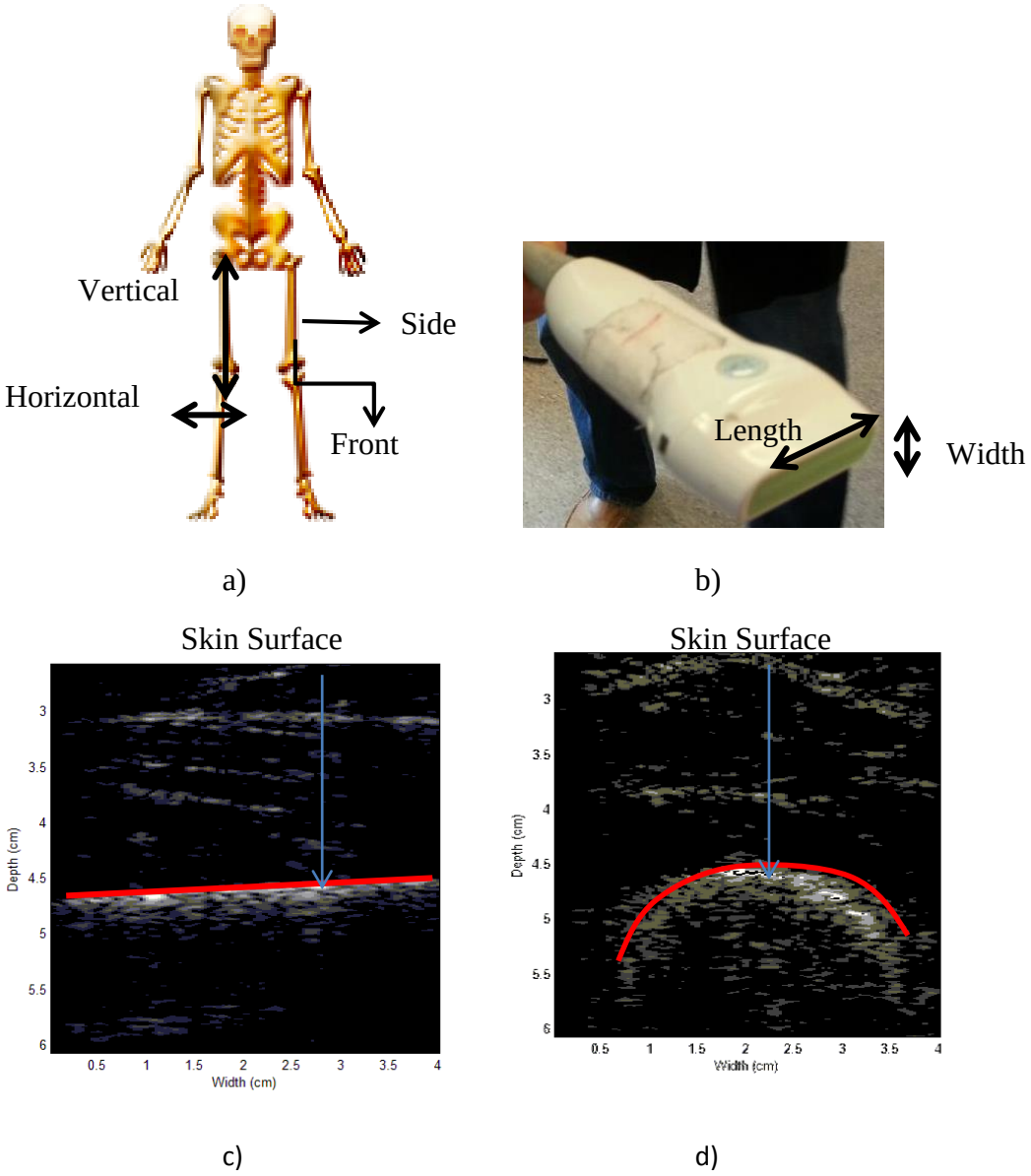

Figure 4.2 Ultrasound images for probe placed on thigh. a) Model representation of human body (Image obtained from [37]) with arrows showing vertical and horizontal allignment of probe as well as front and side of thigh b) The ultrasound probe used in the experiment showing length and width of probe. Ultrasound images showing depth of bone when the probe is placed on thigh with length of probe alligned c) vertically and d) horizontally.

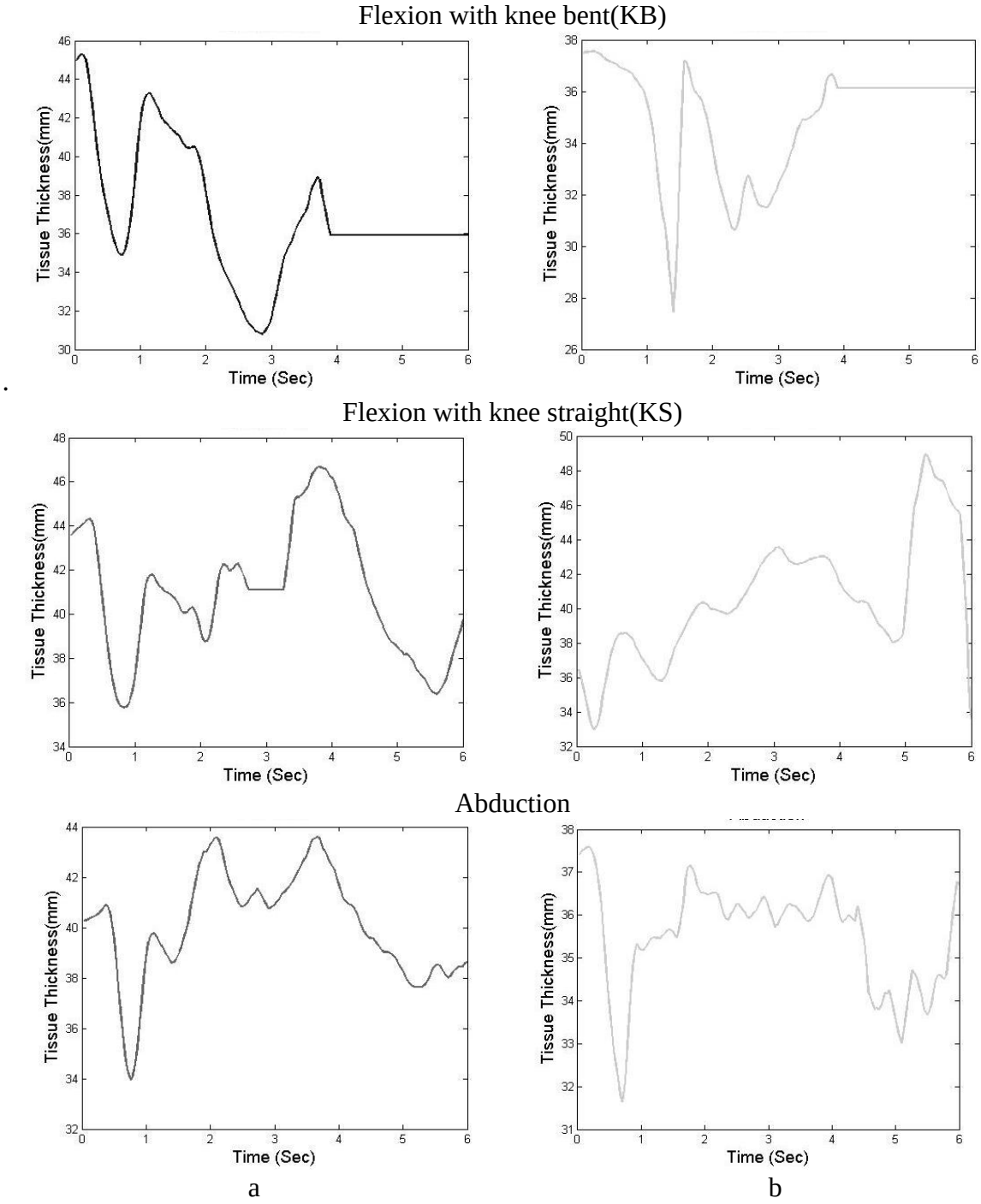

Figure 4.3 Tissue thickness variation obtained from ultrasound for Flexion(KB), Flexion (KS) and Abduction movement with probe placed on the a) front and b) side for one participant

Apart from the contour data obtained from processing ultrasound images in MATLAB and EdgeTrak, the 3D positional information for each marker present in the field of view of *6* cameras were obtained for N frames depending on the duration of each movement type. Coordinate 3D (C3D) data type was explored using btk toolkit in MATLAB to fetch the marker information from VICON blade software.

The figure 4.4 shows the 3D trajectory of *6* markers placed on body while femur is flexed with respect to a stationary pelvis. This trajectory information along with tissue thickness from ultrasound is analyzed in next chapter to evaluate soft tissue artifact and calculate hip joint center using functional algorithm. P_i and Th_i are markers placed on Pelvis and Thigh respectively for i markers ($i = 1$ to 3)

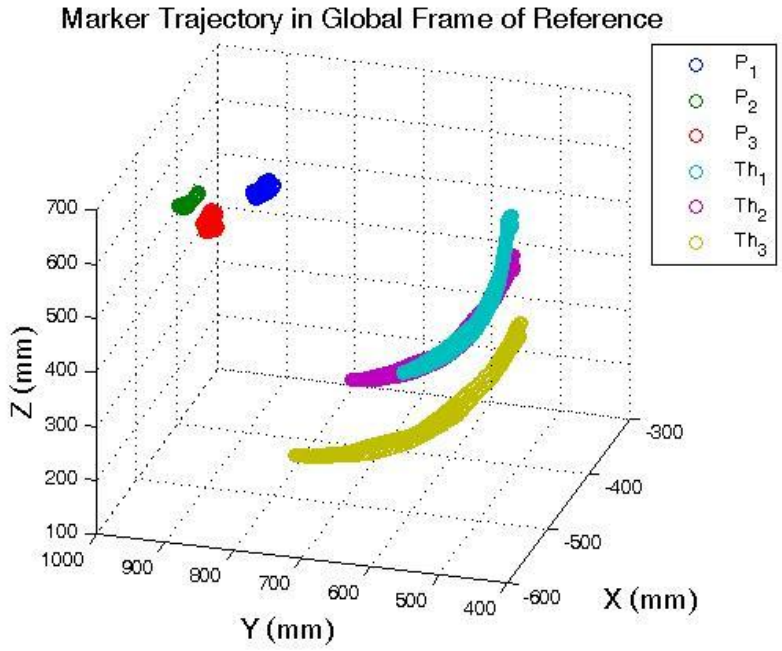

Figure 4.4. Trajectory of three markers on pelvis and three on thigh are shown in global frame of reference with movement Flexion(KB) obtained. The trajectory is an ensemble of position vector obtained over N frames with frame rate of 120 frames per second

Chapter 5. Data Analysis and Results

Based on the procedure described in the previous section, two kinds of data were obtained. The data on change in tissue thickness/ bone depth on thigh were obtained from ultrasound as shown in figure 4.3. Secondly the data on 3D coordinates of all the markers placed on the body were obtained from VICON and converted into a MATLAB readable format using btk toolkit available as a MATLAB binary downloadable from *"https://code.google.com/p/b-tk/wiki/MatlabBinaries"*

Information on change in tissue thickness obtained from ultrasound was analyzed with the joint angles which are in turn calculated using femur and pelvic rotation matrices as described in section 3.2.1. The joint orientation matrix, R_{joint} with respect to pelvic frame of reference was obtained through the orientation matrices R_f and R_p defining the femur and pelvic segments so that for $i = 1$ *to* N frames

$$R_{joint}(i) = {R_p}^{-1}(i) * R_f(i) \tag{18}$$

The angles were determined from rotation matrix obtained by singular value decomposition [48] algorithm with respect to the defined pelvic frame of reference with three markers. For a 3x3 rotation matrix R_{joint} with nine elements as described in Cappozzo et al. [21] joint angle of rotation with respect to a segment are obtained as,

$$alpha = \sin^{-1}(r_{32}) \tag{19}$$

$$beta = \sin^{-1}\left(\frac{r_{31}}{\cos(alpha)}\right) \tag{20}$$

$$gamma = \sin^{-1}\left(-\frac{r_{21}}{\cos(alpha)}\right) \tag{21}$$

Where r_{ij} are the elements of rotation matrix with i^{th} row and j^{th} column. Here ***alpha, beta*** and ***gamma*** are the angle of rotations of femur with respect to pelvis ***X, Y*** and ***Z*** axis. These axes do not have a practical meaning as they are constructed using any three markers on pelvis and hence just represent a frame of reference without any directional significance. Construction of anatomical frame of reference and hence axes was beyond the scope of the study.

From the graphs, figure 5.1, a linear relation was noted for change in tissue thickness with the angle of rotation for Flexion (KB) profile. Tissue thickness at the front of thigh decreases linearly with increase in hip flexion angle. With this information it was assumed that the bone position changes with respect to skin during movement type flexion and hence skin markers do not accurately represent the bone pose. This information obtained from ultrasound can be combined with three dimensional position of probe through VICON to get an estimate of a point on bone in global frame of reference. With this estimated position of bone, we can get the trajectory of markers so that they represent the movement of bone in 3D space rather than that of skin. Hence, soft tissue artifact could be assessed and compensated in a non-invasive manner for each participant

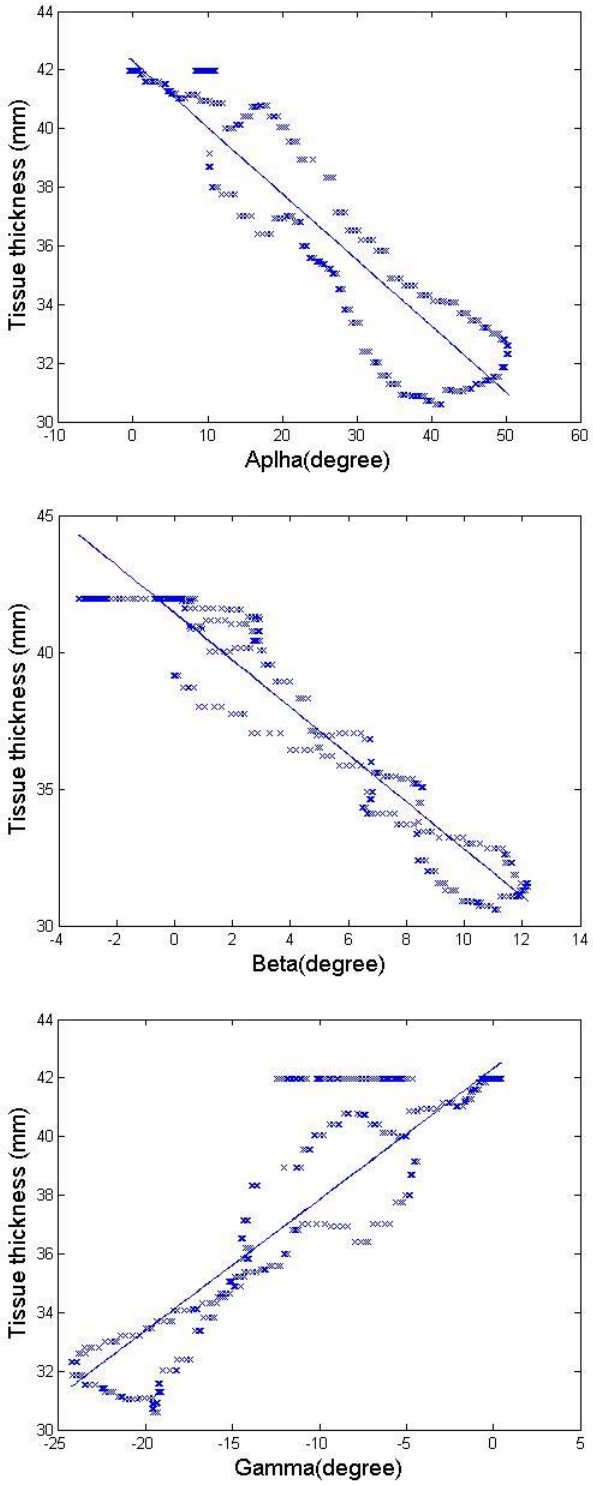

Figure 5.1. Correlation between angle of rotation with change in tissue thickness. Alpha, Beta and Gamma are joint angle of rotation as described in equations *(19),(20)* and *(21)*

5.1 Representation of Soft Tissue Artifact using Bone Trajectory from Ultrasound

In chapter 3, section 3.3.1 we have discussed about the cause of error known as soft tissue artifact in human movement analysis which occurs due to the use of markers placed on skin. This error has been explicitly assessed using invasive techniques. We a need frame of reference fixed to bone to evaluate the amount of marker displacement on skin with respect to underlying bone. The change in shape of marker cluster on the moving segment (thigh) can be estimated using average displacement of three markers on thigh in space with respect to each other as shown in figure 5.2.

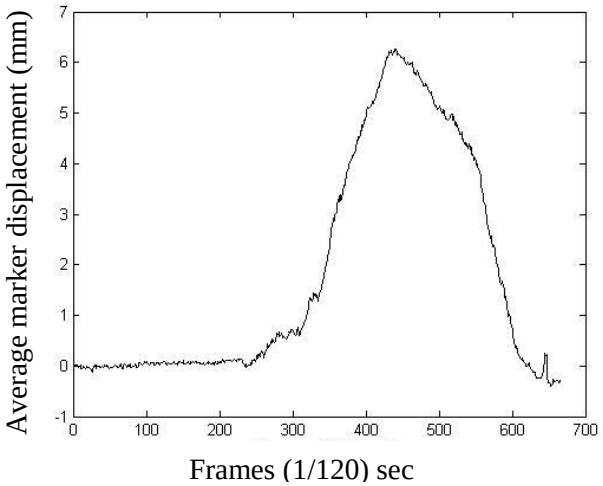

Figure 5.2. Average displacement of three markers on thigh with respect to each other during hip flexion (KB) for one participant.

This gives us the information regarding skin displacement from frames *300* to *600* as the hip is flexed. The maximum movement due to change in shape of markers with respect to

each other is *6 mm*. We are not considering improvement of change in cluster shape in this study. We are concentrating on how thigh markers move with respect to underlying bone.

To get an estimate of how much are these markers moving with respect to underlying bone we obtain a probe's frame of reference defined by three markers on probe as shown in figure 5.3

$$X = |Pr_3 - Pr_1|/norm(Pr_3 - Pr_1) \quad (22)$$

$$Z = crossProduct(|Pr_2 - Pr_1|/norm(Pr_2 - Pr_1), X) \quad (23)$$

$$Y = crossProduct(Z, X)) \quad (24)$$

$$R_{probe} = [X\ Y\ Z] \quad (25)$$

$$O_{probe} = Pr_2 \quad (26)$$

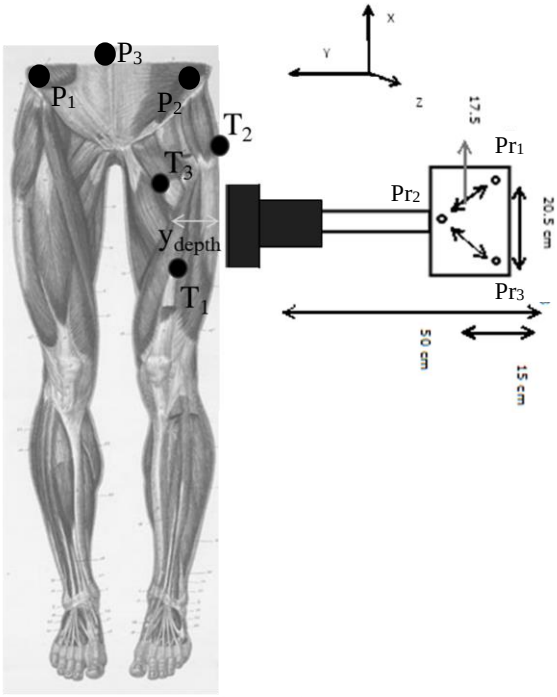

Figure 5.3. A representation of markers on thigh, T_n and pelvis, P_n with ultrasound probe placed on the thigh with markers Pr_n (n = 1 to 3) forming the probe frame of reference (Human thigh image obtained from Anatomy Atlas[4])

The probe frame of reference is such that the image is contained in probe's local $\boldsymbol{XY}$ plane so that $\boldsymbol{Y}$ is the direction perpendicular to the depth of bone and parallel to direction of movement.

In order to find a point to match the bone depth variation, we calculate the centroid of the probe's marker positions and translate it in probe's local $\boldsymbol{Y}$ direction at each time frame

$$Pc = \frac{1}{3} * (Pr_1 + Pr_2 + Pr_3) \tag{27}$$

$\boldsymbol{P_c}$ is the centroid in frame of reference of probe. This centroid is translated by a known distance to reach the surface of the skin. The distance from probe point $\boldsymbol{P_2}$ to skin is 350mm. This is then further translated to match bone depth for each time frame in $\boldsymbol{Y}$ direction. This point is then converted in global frame of reference. The distance between this point on bone and markers on skin should remain constant if the skin markers were rigidly associated with bone. This displacement with respect to neutral position is given in figure 5.4 below.

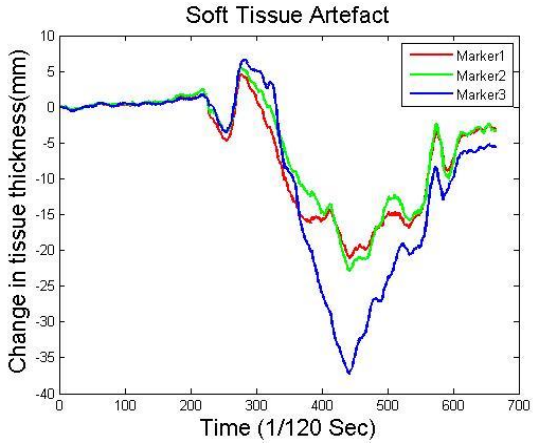

Figure 5.4. Variation of distance between a calculated point on bone and three markers on thigh with respect to neutral position (when participant is standing still)

The markers, T_n, (n = 1 to 3) on thigh, figure 5.3, are now converted into probe's frame of reference using the R_{probe} and O_{probe},

$$T_{probe_n} = R_{probe}^{-1}(T_n - O_{probe}) \quad (28)$$

For each time frame, all three thigh marker positions obtained in probe's frame of reference (T_{probe_n}) are translated in Y direction to match the depth of the bone using *ydepth* obtained from ultrasound synchronized with VICON frames as shown in figure 5.3. These new marker positions are then used to construct a new frame of reference (New_R_f *and* New_O_f) using equations *(22)* to *(26)* with (T_{probe_n} + **[0 *ydepth* 0])** instead of P_n. This frame of reference is considered to be attached to bone rather than skin.

A bone fixed frame of reference is hence calculated by translating all three markers on thigh to match the bone trajectory information and reconstructing the rotation matrix and translation vector from those three points.

The positional artifact depicting the displacement of skin markers in a bone rigid frame of reference as defined by Cappozzo et al. [42] was determined in bone frame of reference as the displacement of thigh markers on skin from their mean position in all time frames

$$pa(i) = m(i) - \frac{1}{N}\sum_{i=1}^{N} m\,(i) \quad (29)$$

Where m is the 3D position of markers and $\frac{1}{N}\sum_{i=1}^{N} m\,(i)$ is the average of position of marker m, over N time frames. The correlation of marker's displacement in bone frame of reference with respect to the flexion angle in pelvic domain is shown in figure 5.5 for three angles in pelvic frame of reference for hip flexion. The average position of all three markers

is calculated so that positional artifact represents the amount of variation of the markers from its average position in a bone fixed frame of reference calculated using the bone depth variation obtained using ultrasound.

Table 5.1 Correlation between joint angle of rotation and marker positional artifact in bone frame of reference

Joint angle of rotation	**Correlation coefficient (r) (P<0.001)**
Alpha	0.84
Beta	0.89
Gamma	-0.85

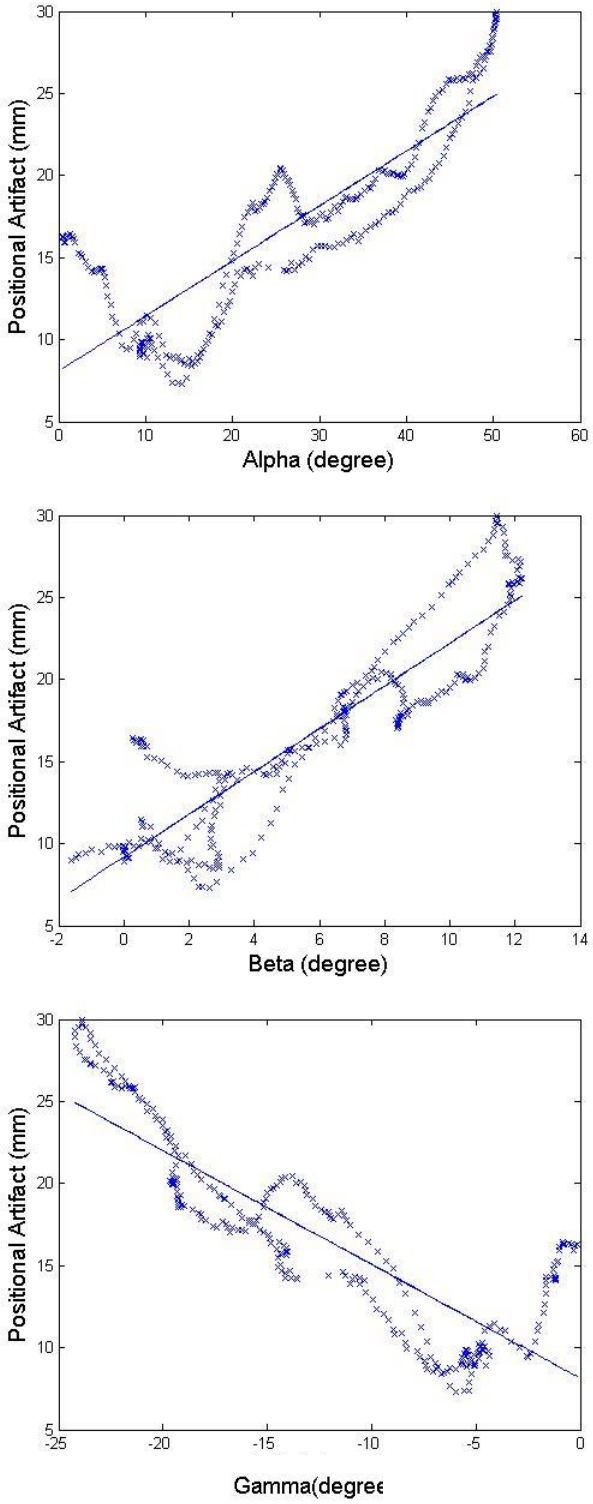

Figure 5.5. Correlation plot between positional artifacts ***(pa)*** as calculated in eq *(29)* in bone frame of reference and joint angle of rotations in pelvic frame of reference.

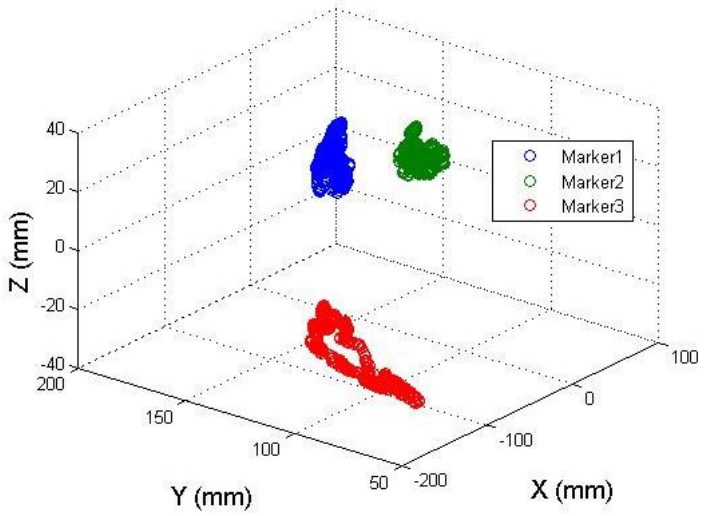

Figure 5.6. 3D representation of skin marker movement in bone frame of reference for three markers on thigh

Soft tissue artifact has been presented as the displacement of markers placed on skin with respect to underlying bone fixed frame of reference. The average movement of markers placed over thigh on skin in bone local frame of reference is found to be an average of *15 mm* which is represented as STA in the figure 5.6.

5.2 Calculation of Functional Hip Joint Center

Calculation of hip joint center using the coordinate transformation method as described in section 3.2.2 requires calculation of rotation matrices for thigh and pelvis each. We have calculated these matrices using two methods namely unit vectors and SVD in section 3.2.1.

The proximal and distal centers, C_p and C_f respectively, were obtained by solving the equation in least square approach using MATLAB

$$\begin{bmatrix} R_{f_1} - R_{p_1} \\ \cdot \\ \cdot \\ R_{f_N} - R_{p_N} \end{bmatrix} \begin{bmatrix} C_f \\ C_p \end{bmatrix} = \begin{bmatrix} O_{p_1} - O_{f_1} \\ \cdot \\ \cdot \\ O_{p_N} - O_{f_N} \end{bmatrix}$$

R_f, R_p are rotation matrices and O_f, O_p are translation vectors for the distal and proximal segment respectively. $i = 1$ to N is the instance of time frame recorded by VICON

The probe's frame of reference was constructed using the equations *(22) to (26)* with markers placed on probe. The Y component points towards the direction of change in tissue thickness. The thigh markers were transformed in probe's frame of reference using the transformation equation (28) and translated by amount of tissue thickness to construct a new frame of reference (New_R_f *and* New_O_f) for thigh from the translated marker positions.

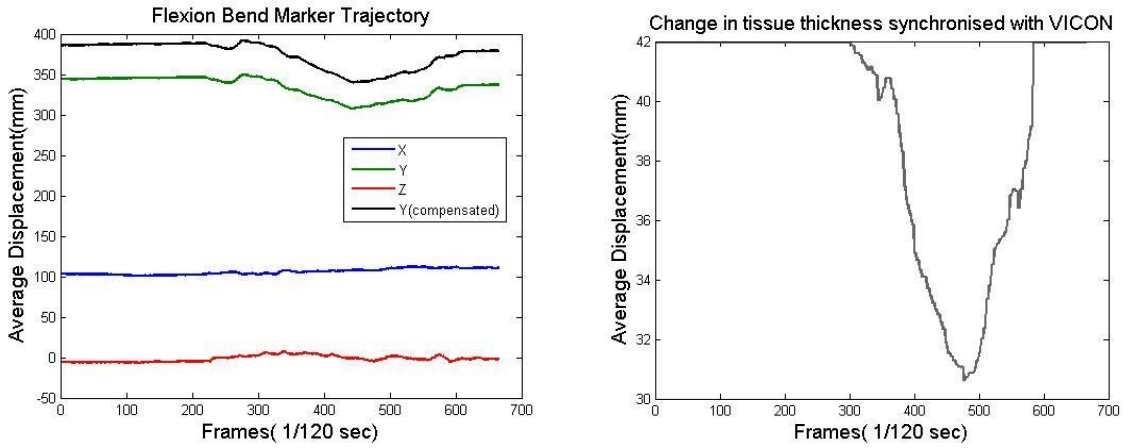

Figure 5.7. a) Average displacement of markers on skin placed on thigh in probe's frame of reference b) change in soft tissue thickness synchronized with VICON.

In figure 5.8 (a) the plot in black is the average of $\boldsymbol{Y}$ component of the thigh markers movement in probes frame of reference after incorporation of tissue thickness variation shown in figure 5.8 (b). The movements in $\boldsymbol{X}$ and $\boldsymbol{Z}$ directions are small (*3.2 mm* and *4.07 mm* respectively) indicating the rigidity of probe's frame of reference with femur. In $\boldsymbol{Y}$ the average movement expressed as absolute displacement from first frame is *11.16 mm.*

The marker positions calculated with bone trajectory information is represented as $\boldsymbol{Th_{bone}}$ in the figure 5.9 below. Hip joint center is now calculated using the SCoRE [20]**Error! eference source not found.** algorithm with the raw set of thigh marker trajectory and with the new trajectory obtained through ultrasound tissue thickness information.

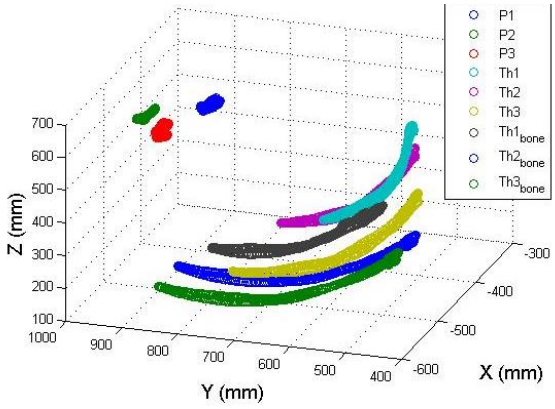

Figure 5.8. Trajectory made by position of three markers placed on each body segment pelvis (P_n), thigh(Th_n) and three markers calculated with bone pose estimation ($Th_{(n)bone}$) are shown in global frame of reference

.

Using the position of thigh markers obtained after the translation in probe's local frame of reference for soft tissue thickness change, the SVD algorithm [48] was used to calculate the orientation New_R_f *and* position New_O_f for both segments in motion and applied to SCoRE to get the hip joint center in proximal and distal segments.

The euclidean distance between C_p and C_f were calculated as SCoRE Residual [36] as described in section 3.2.3

$$r = |C_p - C_f|$$

This is calculated for time frames identified for the duration of the movement giving maximum correlation with the ultrasound sunchronized data and presented below for two cases for each participant. Firstly with the rotation matrices obtained from raw data marker trajectory obtained directly from VICON (R_f, R_p) and secondly, with recalculated marker positions for thigh after tissue thickness information from ultrasound was imposed (New_R_f).

Figure 5.10 and 5.11 show the frequency distribution and spread, resp., of the error over time period in which the participant was flexing the hip. The error was reported in pelvic frame of reference for the purpose of comparision in a fixed anatomical frame of reference.

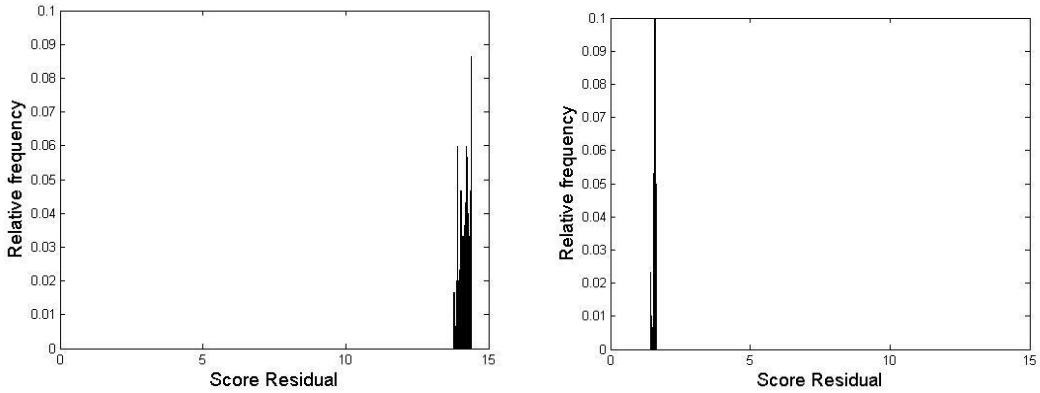

a b

Figure 5.9. Score Residual obtained in pelvic frame of reference from: a) marker position on skin b) bone movement compensated thigh marker trajectory

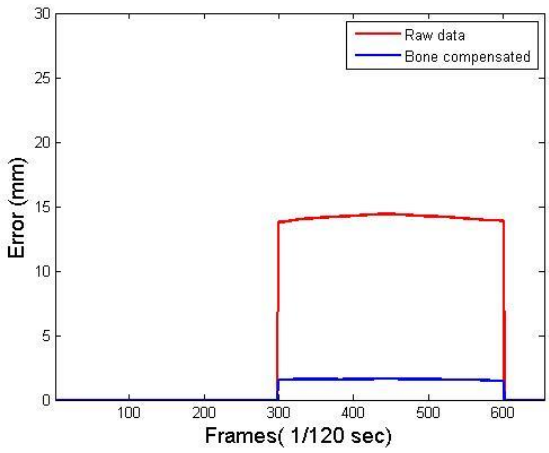

Figure 5.10. The error calculated as distance between proximal and distal centers obtained over time frames while hip is flexed for one participant.

The center location along with skin marker and bone trajectory is shown in the figure 5.12 below in global ***ZY***, ***ZX*** and ***YX*** planes respectively. C_1 and C_2 are centers calculated with raw data, without and with SVD algorithm used for calculation of rotation matrix respectively. The absolute distance between these centers is *5.75* mm. C_3 is the center calculated with bone trajectory from new markers using SVD. It has been shown [29] that with the use of SVD, the error associated with change in shape of cluster of markers is lesser. Hence, for comparision amongst participants, SVD method is used for calcultation of rotation matrices. In figure 5.12, ***Y*** is the direction defining superior / inferior (Up as positive direction) and ***XZ*** is the transverse plane.

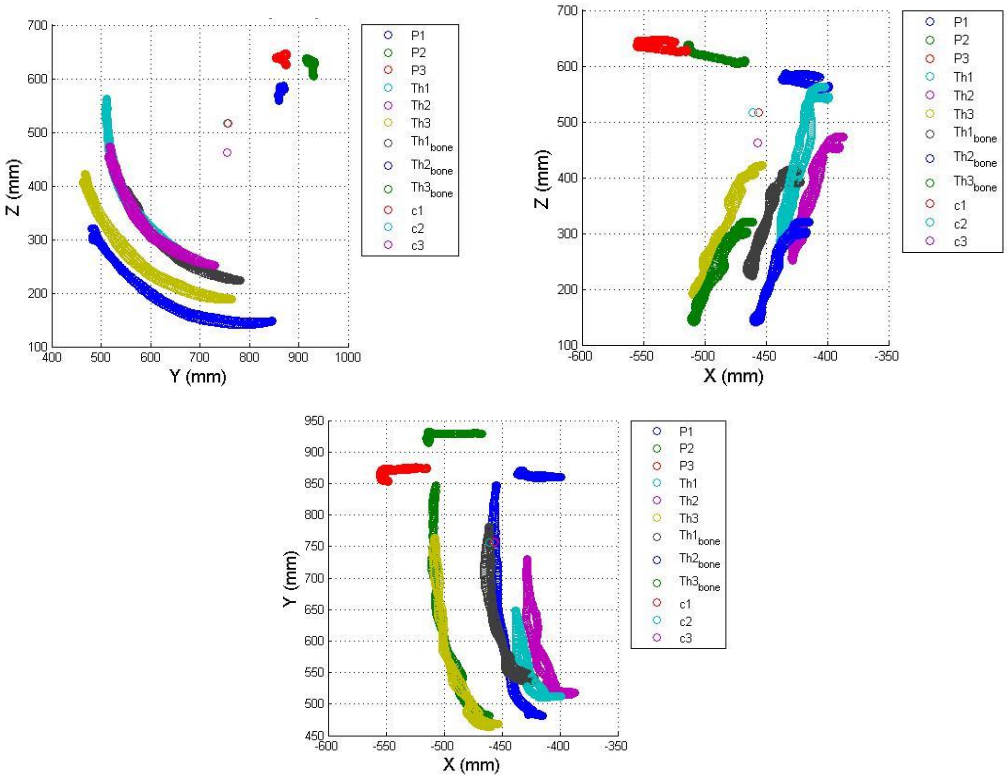

Figure 5.11. Trajectory of markers on skin(Pelvis: P_1, P_2, P_3 , Thigh: Th_1, Th_2, Th_3) and calculated markers on bone(Th_{1bone} , Th_{2bone}, Th_{3bone}) in global frame of reference along with position of calculated hip joint center (c_1, c_2, c_3)

For the purpose of testing repeatability, the algorithm was tested on flexion (KB) movement performed twice by the same participant, as shown in figure 5.13, for whom ultrasound data was available from the first movement recording. Proximal and distal centers are an average of pelvic and thigh centers determined in pelvic frame of reference respectively, for N time frames using SCoRE algorithm.

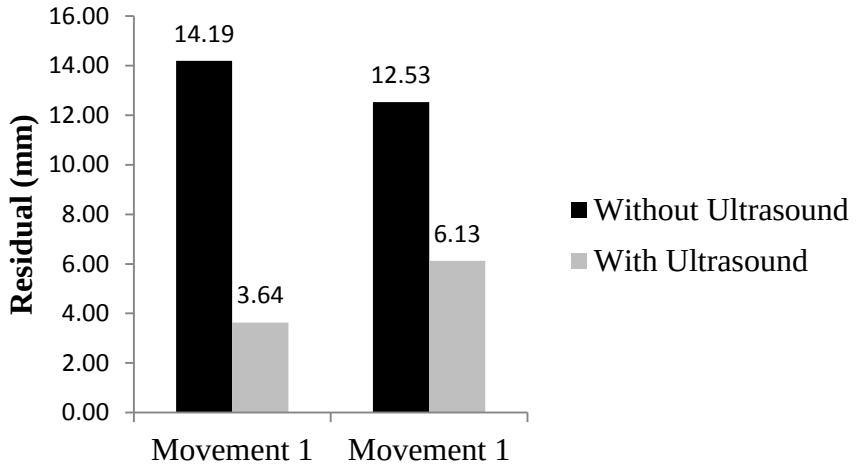

Figure 5.12. Comparison of residual as distance between proximal and distal centers calculated by coordinate transformation algorithm with markers on skin and bone for one participant with same movement performed twice.

As per our hypothesis, after performing a detailed analysis on the participant's data with maximum correlation, the algorithm was extended to other participants. Other participants did not have an acceptable correlation ($r > 0.8$) between skin marker and bone movement over all frames of flexion (Table 4.2). Hence the time frames were acknowledged for all participants with correlation value $r > 0.8$, starting at the begining of motion identified through synchronization as described earlied. The SCoRE algorithm was then applied over those identified time frames for all participants with rotation matrices calculated using skin markers and new calculated markers containing bone trajectory information. The results are shown in figure 5.14. where the legends : Without and With Ultrasound, represent

calculations through skin markers and new calculated markers containing bone trajectory information, respectively.

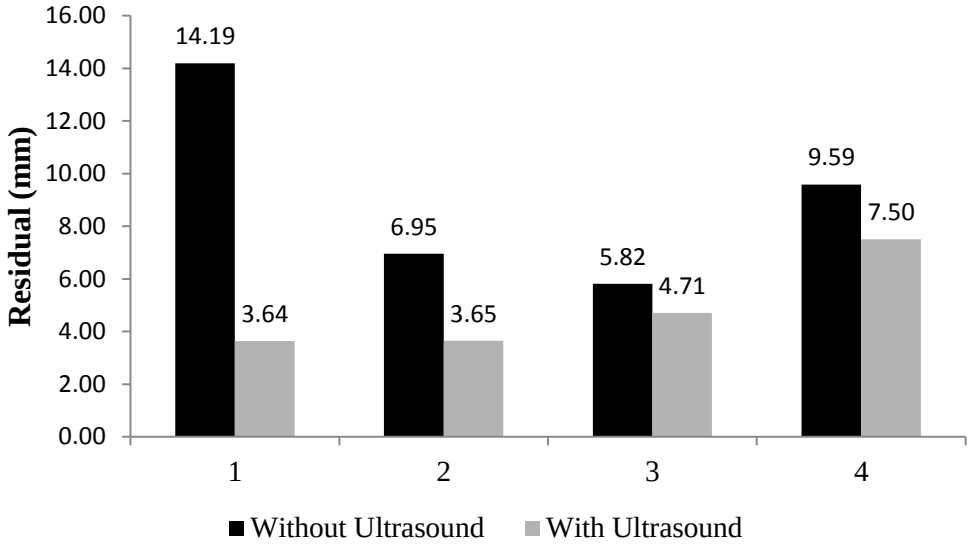

Figure 5.13. Comparison of residual as distance between proximal and distal centers calculated by coordinate transformation algorithm with markers on skin and bone for four participants.

Chapter 6. Discussion

We have suggested a novel idea of integrating ultrasound imaging with human motion analysis in order to improve the estimate of bone pose reconstruction from markers placed on skin. This method is a cost effective and realistic approach towards improving the existing algorithms. Here we have proposed and demonstrated the feasibility of combining two imaging modalities which can be utilized in numerous applications which require precise identification of instant center of rotation. We have shown the applicability on hip joint but it might be applicable to other similar joints which could be modeled as ball and socket. An improvement of algorithm (SCoRE) for estimating hip joint center using this method has been suggested using the bone depth information. The skin markers placed on thigh are translated in space by the amount of bone depth variation during hip flexion in order to make the markers follow bone movement trajectory and hence provide a better estimate of its position in 3D space than current methods.

We have analyzed the motion type flexion with knee in bent position to evaluate the dependency of the skin marker displacement with respect to underlying bone using ultrasound based bone trajectory information. This method was based on the fact that if probe position is known in 3D laboratory space and the image plane contains the information of bone position, the estimate of a point on bone could be made. This gave us a bone fixed frame of reference non-invasively and the displacement of markers on skin with respect to this frame of reference could be calculated.

Functional hip joint center technique with coordinate transformation algorithm was tested on participants. In this method it is assumed that a constant distance is maintained from joint

center to marker coordinates in each local segment. Bone trajectory information was imposed on skin markers for better reconstruction of bone and hence the center. Distance between the proximal and distal centers was calculated to test the accuracy of the algorithm. This method has been established previously [36] to test the accuracy of the results. To elaborate more on the measurement of accuracy as a residual of calculated proximal and distal centers, Ehrig et al. [36] established SCoRE residual as a measure of error. They proved that this measure of distance between calculated proximal and distal centers through SCoRE coordinate transformation algorithm is proportional to the error between the calculated and actual centers and can provide an estimate of accuracy of algorithm in case ground truth is not available. Hence we have used this measure as an estimate of accuracy in our research.

The algorithm was tested for one participant at first for a detailed analysis. The positions of markers were reconstructed in pelvic fixed frame of reference and the error was brought down from *14.19 mm* to *3.64 mm* by reconstructing the bone position with use of ultrasound data for this participant. When applied to other participants for the time frames with maximum correlation value, the error value was brought down significantly with our method. The mean error value is brought down by *46.65%* from *9.13 mm* with standard deviation *3.71 mm* with skin marker data to *4.87 mm* with standard deviation *1.82 mm* with bone trajectory imposition. Student's t test was performed to test the difference of means with unequal variance between the results of two methods to support the alternative hypothesis that the error was significantly lesser with our method at a 5% significance level. Also the absolute distance between calculated centers of rotation between the two methods was close to *30 mm* which is in the range of agreement with the study based on X-Ray by

Bell et al. [14]. We have utilized the well-established algorithm of coordinate transformation to determine the estimate of HJC through external markers using suggested movements and cluster of markers. Hence it is assumed that the calculated proximal and distal centers will be close to the actual and that the SCoRE residual would provide a check on accuracy as established before.

The quantitative analysis was limited by the errors due to manual handling of probe which might pose pressure based variation in different participants. Ultrasound data was noisy and some of the frames were missing due to misplacement of probe during the motion. These frames were manually identified and the value was treated as an outlier with mean value treatment. Out of 4 motion types, only Flexion (KB) had a significant ($P < 0.001$) correlation between ultrasound and VICON determined frames to reconstruct the bone trajectory information for the entire motion in accordance with previous studies [38]. The probe attachment was heavy making it difficult for participant to hold it rigidly during the motion. Also, synchronization is done based on manual observation and analysis of graph based data. For all the profiles, few data points are against the observed trend which is assumed to be due to excessive pressing of ultrasound probe which alters the tissue thickness and change is not observed. The change is observed if only the probe was held neutrally without pressing the skin. Another limitation is evaluation of one dimensional bone variation rather than 3D which is available from studies with bone pins which comes with its own drawback of being invasive. Hence in this qualitative analysis, only one participant's data was fully analyzed to present the proof of concept for visualization of the idea to use ultrasound as an ad hoc exercise for accurate bone pose estimation.

VICON system accuracy was assessed by measuring the distance between two markers rigidly attached onto the probe's attachment. Its dynamic accuracy was tested as the amount of variation in this distance compared to the actual distance between markers while the probe was moved in space. The accuracy was an average of 0.44 ± 0.04 *mm* standard deviation. Propagation of this error in measurement could lead to certain inaccuracies in measurement of HJC.

Correlation between angle or rotation and positional artifact has been shown in previous studies [38] and similar relation is found in our experiments. One of the participants showed correlation with correlation coefficient r greater than *0.8* between angle of rotation and change in tissue thickness with $P < 0.001$ for the entire duration of motion. This data was chosen for further analysis to establish and test the algorithm for whole duration of flexion back to neutral position. This correlation value for other participants was less than *0.8* for the whole duration for flexion movement. Consequently, for the application of SCoRE algorithm, the continuous time frames were identified for other participants for whom the correlation value was > 0.8 and then the algorithm was implemented on that restricted data to calculate the hip joint center using new reconstructed marker positions for the identified frames.

We have provided a qualitative analysis of soft tissue artifact by reconstructing orientation and position of bone with the help of markers placed on probe and the variation of bone during the movement in 1D. As the angle of rotation increases in global XY plane for the flexion motion in pelvic frame up to 50° the tissue thickness decreases by 23%. We present a possibility to determine the subject and task specific bone trajectory information through ultrasound which could possibly be integrated with the algorithm of Alexander et al. [38] to

determine interval based deformation to accommodate for skin movement artifact. Figure 5.1 shows a correlation plot between the angle of rotation in pelvic frame of reference and the change in tissue thickness over bone synchronized over time frames. This information, along with the dependency of positional artifact calculated in equation *(29)* (figure 5.5), indicates a possibility to model the soft tissue artifact for error compensation using the information on bone trajectory non-invasively in future. The coefficient of regression fit between these quantities can be analyzed further in order to model the STA with ample number of participants in the study. This is left as a future scope of the research.

An attempt was made to improve HJC calculation from skin markers with information about bone movement and its position with respect to global coordinate system from ultrasound data synchronized with 3D positional VICON data. The markers placed on skin gave an estimate of HJC which was medial and anterior to the one calculated with the estimation of bone pose from ultrasound. Due to the lack of Gold standard data, the validation of the accuracy of this method cannot be done. The SCoRE residual [36], which has been established to give an estimate of error compared close to gold standard, was significantly reduced ($P<0.05$) although our main aim was to get a better estimate of the center rather than improvement of algorithm used to calculate the same.

The suggested method of incorporating bone trajectory information to recalculate marker positions was tested on two trials by one participant and the average distance between the centers from skin and bone based markers was *31.02 mm* and *30.44 mm* for two trials respectively. The difference of means between these two trials was not significant based on t test hypothesis done using MATLAB. The bone trajectory information extracted from one data point for flexion (KB) profile was applied on the second trial in which ultrasound data

was not available and the results came out to be close enough. This provides the repeatability information in the experiment. The SCoRE residual decreased for all participants when it was calculated with markers reconstructed with bone trajectory information. One of the reasons for maximum reduction in participant 1 could be due to the use of maximum number of frames for entire flexion motion. This gives better range of motion for calculation of HJC. For other participants only a subset of time frames during the movement was used such that for those frames, the correlation (r) between skin and marker movement was greater than the set threshold of *0.8*. Hence the reduction in error is lesser but still a significant value indicating the usability of algorithm with adequate range of motion information.

One plane motion, flexion, was evaluated because only one dimension information regarding the change in depth of bone was available through the ultrasound. This might tend to give more error than multi planar motion as evaluated in previous studies using a pivoting algorithm [25]. Although, it was found in a study that functional hip joint center calculation algorithms perform similarly in single plane motion as long as the range of motion is adequate [65]. We have utilized maximum range of motion in participant's caliber in the study. Also, the FAI occurs at anterio-superior region of hip joint which is affected by the flexion movement and hence there is a need to evaluate this motion type for the hip abnormality under consideration. Other non-invasive studies [50] have assessed the effects of the soft tissue artifact using fluoroscopy, but they have not suggested a compensation technique. Interpolation method described in [51] is complicated and does not include subject specific traits. Hence ultrasound can be feasibly integrated with motion analysis to track the subject specific traits to solve the problem of STA non-invasively.

The future studies will attempt towards measuring three dimensional bone displacements in multi-planar movements with wearable ultrasonic sensors which do not hinder the natural movement. The limitations of handling the probe manually and unexpected amount of pressure given to the ultrasound probe are expected to over-come by attaching the probe through a foam based attachment rigidly onto the thigh. The time synchronization between the two imaging modalities can be improved by improvising automatic synchronization based on time stamps or an external trigger based circuit. Number of participants will be considerably increased in order to perform statistical analysis on the coefficient of linear regression between angle or rotation and positional artifact. In the end, the validation of this concept with a gold standard data would be needed for use in clinical settings.

Abbreviations

CT	Computed Tomography
FAI	Femoroacetabular Impingement
GT	Greater Trochanter
HJC	Hip Joint Center
LASIS	Left Anterior Superior Illiac Spine
LE	Lateral Epicondyle
LPSIS	Left Posterior Superior Illiac Spine
ME	Medial Epicondyle
MRI	Magnetic Resonance Imaging
OA	Osteoarthritis
RASIS	Right Anterior Superior Illiac Spine
ROM	Range of movement
RPSIS	Right Posterior Superior Illiac Spine
SCoRE	Symmetric Center of Rotation Estimate
STA	Soft Tissue Artifact

References

[1] Bonneau N, Gagey O, Tardieu C. Biomechanics of the human hip joint. Computer Methods In Biomechanics & Biomedical Engineering .September 2012;15:197-199.

[2] Wu G, Siegler S, Allard P, Kirtley C, Leardini A, Rosenbaum D, Whittle M, D'Lima DD, Cristofolini L, Witte H, Schmid O, Stokes I. ISB recommendation on definitions of joint coordinate system of various joints for the reporting of human joint motion—part I: ankle, hip, and spine. Journal of Biomechanics. April 2002;35(4):543-548.

[3] Byrne DP, Mulhall KJ and Baker JF. Anatomy & Biomechanics of the Hip. The Open Sports Medicine Journal, 2010, 4, 51-57

[4] D'Alessandro MP and Bergman RA, Anatomy Atlases, http://www.anatomyatlases.org. Retrieved on July 2013 [Online]

[5] Field D, Hutchinson JSO & Redmond A. Field's lower limb anatomy, palpation, and surface markings. Edinburgh: Churchill Livingstone Elsevier, 2008:15-55

[6] Field D, Hutchinson JSO & Redmond A. Field's lower limb anatomy, palpation, and surface markings. Edinburgh: Churchill Livingstone Elsevier, 2008:57-107

[7] Ball-and-socket-joint. (n.d.). In Encyclopaedia Britannica Online. Retrieved on April 2013 from http://www.britannica.com/EBchecked/topic/50423/ball-and-socket-joint [Online]

[8] O'Rahilly R, Muller F, Carpenter S & Swenson R. Basic Human Anatomy - Chapter 12: The bones of the lower limb. Retrieved on April 2013 from http://www.dartmouth.edu/~humananatomy/part_3/chapter_12.html [Online]

[9] DK books. Retrieved on April 2013 http://www.clipart.dk.co.uk/379/subject/Biology/Ball_and_socket [Online]

[10] Chapter 7. Functional Anatomy of the Hip Joint. 237-250. Retrieved on April 2013 from https://catalog.ama-assn.org/MEDIA/ProductCatalog/m890153/%20Function%20%20Anatomy%20Ch%207.pdf [Online]

[11] Sun H, Inaoka H, Fukuoka Y, Masuda T, Ishida A, Morita S. Range of motion measurement of an artificial hip joint using CT images. Medical & Biological Engineering & Computing. December 2007;45(12):1229-1235.

[12] Kang MJ, Sadri H, Moccozet L, Magnenat-Thalmann N, Pierre Hoffmeyer: Accurate simulation of hip joint range of motion, Proc. of IEEE Computer Animation 2002:215-219.

[13] Cappozzo A, Gait analysis methodology, Human Movement Science, March–June 1984:3(1-2):27-50

[14] Bell AL, Brand RA, Pedersen DR, Prediction of hip joint centre location from external landmarks, Human Movement Science, February 1989, 8(1)

[15] Fessy MH, N'Diaye A, Carret JP, Fischer LP. Locating the center of rotation of the hip. Surg Radiol Anat. 1999;21(4):247-50
[16] Camomilla V, Cereatti A, Vannozzi G, Cappozzo A. An optimized protocol for hip joint centre determination using the functional method. Journal of Biomechanics. June 2006;39(6):1096-1106
[17] Piazza S, Erdemir A, Okita N, Cavanagh P. Assessment of the functional method of hip joint center location subject to reduced range of hip motion. Journal of Biomechanics March 2004;37(3):349-356.
[18] Begon M, Monnet T, Lacouture P. Effects of movement for estimating the hip joint centre. Gait & Posture. March 2007;25(3):353-359.
[19] Leardini A, Cappozzo A, Catani F, Toksvig-Larsen S, Petitto A, Sforza V, Cassanelli, G, Giannini S.Validation of a functional method for the estimation of hip joint centre location. Journal of Biomechanics, 1999, 32 (1), 99-103
[20] Ehrig R, Taylor W, Duda G, Heller M. A survey of formal methods for determining the centre of rotation of ball joints. Journal of Biomechanics .December 22, 2006;39(15):2798-2809
[21] Cappozzo A, Della Croce U, Leardini A, Chiari L. Human movement analysis using stereophotogrammetry: Part 1: theoretical background. Gait & Posture .February 2005;21(2):186-196.
[22] Chiari L, Croce U, Leardini A, Cappozzo A. Human movement analysis using stereophotogrammetry: Part 2: Instrumental errors. Gait & Posture .February 2005;21(2):197-211
[23] Leardini A, Chiari L, Croce U, Cappozzo A. Human movement analysis using stereophotogrammetry: Part 3. Soft tissue artifact assessment and compensation. Gait & Posture. February 2005;21(2):212-225
[24] Della Croce U, Leardini A, Chiari L, Cappozzo A. Human movement analysis using stereophotogrammetry: Part 4: assessment of anatomical landmark misplacement and its effects on joint kinematics. Gait & Posture. February 2005;21(2):226-237
[25] Siston R, Delp S. Evaluation of a new algorithm to determine the hip joint center. Journal of Biomechanics January 2006;39(1):125-130
[26] Cereatti A, Donati M, Camomilla V, Margheritini F, Cappozzo A. Hip joint centre location: An ex vivo study. Journal of Biomechanics May 11, 2009;42(7):818-823.
[27] De Momi E, Lopomo N, Cerveri P, Zaffagnini S, Safran M, Ferrigno G. In-vitro experimental assessment of a new robust algorithm for hip joint centre estimation. Journal of Biomechanics May 29, 2009;42(8):989-995.
[28] Lopomo N, Sun L, Zaffagnini S, Giordano G, Safran M. Evaluation of formal methods in hip joint center assessment: An in vitro analysis. Clinical Biomechanics. March 2010;25(3):206-212

[29] Peters A, Baker R, Morris M, Sangeux M. A comparison of hip joint centre localisation techniques with 3-DUS for clinical gait analysis in children with cerebral palsy. Gait & Posture June 2012;36(2):282-286.
[30] Sangeux M, Peters A, Baker R. Hip joint centre localization: Evaluation on normal subjects in the context of gait analysis. Gait & Posture. July 2011;34(3):324-328.
[31] Heller M, Kratzenstein S, Ehrig R, Wassilew G, Duda G, Taylor W. The weighted optimal common shape technique improves identification of the hip joint center of rotation in vivo. Journal of Orthopaedic Research October 2011;29(10):1470-1475.
[32] Bouffard V, Begon M, Champagne A, Farhadnia P, Vendittoli P, Lavigne M, and Prince F, Hip joint center localisation: A biomechanical application to hip arthroplasty population World J Orthop. 2012 August 18; 3(8): 131–136
[33] Peters A, Baker R, Sangeux M. Validation of 3-D freehand ultrasound for the determination of the hip joint centre. Gait & Posture . April 2010;31(4):530-532.
[34] Gamage S, Lasenby J. New least squares solutions for estimating the average centre of rotation and the axis of rotation. Journal of Biomechanics. January 2002;35(1):87-93.
[35] Halvorsen K. Bias compensated least squares estimate of the center of rotation. Journal of Biomechanics . July 2003;36(7):999-1008.
[36] Ehrig R, Heller M, Kratzenstein S, Duda G, Trepczynski A, Taylor W. The SCoRE residual: A quality index to assess the accuracy of joint estimations. Journal of Biomechanics April 29, 2011;44(7):1400-1404.
[37] Image human skeleton Retrieved on May 2013 from http://3.bp.blogspot.com/-GWlMb5oZuhM/UJbluiVoIkI/AAAAAAAAGGg/ftTD51aPVAI/s1600/CG91.png [Online]
[38] Alexander EJ, Andriacchi TP, Correcting for deformation in skin-based marker systems, Journal of Biomechanics. March 2001,34(3),:355-361
[39] Ryu T, Choi HS, Chung MK, Soft tissue artifact compensation using displacement dependency between anatomical landmarks and skin markers – a preliminary study, International Journal of Industrial Ergonomics, January 2009, 39(1) , 152-158
[40] Akbarshahi M, Schache AG, Fernandez JW, Baker R, Banks S, Pandy MG, Non-invasive assessment of soft-tissue artifact and its effect on knee joint kinematics during functional activity, Journal of Biomechanics, May 2010, 43(7):1292-1301
[41] Heller M, Kratzenstein S, Ehrig R, Wassilew G, Duda G, Taylor W. The weighted optimal common shape technique improves identification of the hip joint center of rotation in vivo. Journal of Orthopaedic Research. October 2011;29(10):1470-1475
[42] Cappozzo A, Catani F, Leardini A, Benedetti M G, Della Croce U. Position in space of bones during movement Clin. Biomech.1996.11(2):90- 100

[43] Speirs AD, Benoit DL, Beaulieu ML, Lamontagne M, Beaule P. The Accuracy of the Use of Functional Hip Motions on Localization of the Center of the Hip HSS Journal 01/2012; 8:192-197.

[44] Hsu P, Prager R, Gee A, Treece G. Real-Time Freehand 3D Ultrasound Calibration. Ultrasound In Medicine & Biology .February 2008;34(2):239-251

[45] Treece GM, Lindop JE, Gee AH, Prager RW, Freehand Ultrasound Elastography with a 3-D Probe, Ultrasound in Medicine & Biology, March 2008, 34(3):463-474

[46] Fry N, Childs C, Eve L, Gough M, Robinson R, Shortland A. Accurate measurement of muscle belly length in the motion analysis laboratory: potential for the assessment of contracture. Gait & Posture .April 2003;17(2):119.

[47] Li M, Kambhamettu C, and Stone M. Automatic contour tracking in ultrasound images. Clinical Linguistics and Phonetics. 2005.19(6-7); 545-554.

[48] Inge Soderkvist, Per-Ake Wedin, Determining the movements of the skeleton using well-configured markers, Journal of Biomechanics. December 1993.26(12):1473-1477

[49] Andriacchi T, Alexander E. A point cluster method for in vivo motion analysis: Applied to a study of knee kinematics. Journal of Biomechanical Engineering. December 1998;120(6):743.

[50] Tsai T, Lu T, Kuo M, Lin C. Effects of soft tissue artifacts on the calculated kinematics and kinetics of the knee during stair-ascent. Journal of Biomechanics. April 7, 2011;44(6):1182-1188

[51] Dumas R, Cheze L. Soft tissue artifact compensation by linear 3D interpolation and approximation methods. Journal of Biomechanics. September 18, 2009;42(13):2214-2217.

[52] Functional Anatomy of Hip Joint. State University of New York. Retrieved on April 2013 from http://www.upstate.edu/cdb/education/grossanat/limbs7.shtml [Online]

[53] Image Planes of movement. Retrieved on April 2013 from http://nextlevelstrengthandfitness.com/wp-content/uploads/2010/09/planes-of-movement.jpg [Online]

[54] Jager M, Wild A, Westhoff B and Krauspe R .Femoroacetabular impingement caused by a femoral osseous head–neck bump deformity: clinical, radiological, and experimental results. Journal of Orthopaedic Science , January 2004. 9(3): 256-263

[55] Filigenzi JM, and Bredella MA. MR imaging of femoroacetabular impingement. Applied Radiology. April 2008.12-19

[56] Kennedy MJ, Lamontagne M, Beaule PE .Femoroacetabular impingement alters hip and pelvic biomechanics during gait Walking biomechanics of FAI. Gait & Posture .2009.30. 41–44

[57] Lamontagne M, Kennedy MJ, Beaule PE. The Effect of Cam FAI on Hip and Pelvic Motion during Maximum Squat. Clin Orthop Relat Res . November 2009.467:645–650

[58] MacDonald SJ, Garbuz D, Ganz R. Clinical evaluation of the symptomatic young adult hip. Semin Arthroplasty .1997.8:3-9
[59] Banerjee P & Mclean CR. Femoroacetabular impingement: a review of diagnosis and management Curr Rev Musculoskelet Med .2011.4:23–32
[60] Gay DP, Desser DR, Parks BG, and Boucher HR. Sciatic Nerve Injury in Total Hip Resurfacing The Journal of Arthroplasty .2010.25(8).1295-1300
[61] Powers CM. The Influence of Abnormal Hip Mechanics on Knee Injury: A Biomechanical Perspective Journal of orthopaedic & sports physical therapy .February 2010.40(2):42-51
[62] Beaule PE, Zaragoza E, Motamedi K, Copelan N, Dorey FJ. Three-dimensional computed tomography of the hip in the assessment of femoroacetabular impingement Journal of Orthopaedic Research .March 2005.23:1286-1292
[63] Meyer DC, Beck M, Ellis T, Ganz R, Leunig M. Comparison of six radiographic projections to assess femoral head/neck aspherecity. Clin Orthop Relat Res.; 2006. 445:181–185
[64] Leunig M, Robertson WJ, Ganz R. Femoroacetabular Impingement: Diagnosis and Management, Including Open Surgical Technique .Open Tech Sports Med .2007.15:178-188
[65] Piazza SJ, Okita N, Cavanagh PR, Accuracy of the functional method of hip joint center location: effects of limited motion and varied implementation, Journal of Biomechanics. July 2001.34(7):967-973

Publications by Author

1. Swati Upadhyaya, WonSook Lee, Zhen Qu, Yuu Ono, Chris Joslin "Use of Ultrasound to Track Bone Trajectory for Human Motion Analysis" *International Journal of Systems, Algorithms and Applications, ICRASE India13* , April 2013, ISBN : 978-81-923541-0-7, pp 52-55
2. Swati Upadhyaya, WonSook Lee "Survey of formal methods of Hip Joint Center calculation in human studies" *APCBEE Procedia (Journal under Elsevier, ISSN: 2212-6708), ICBET 13 Denmark*, May 19-20, 2013
3. Swati Upadhyaya, WonSook Lee, Zhen Qu, Yuu Ono, Chris Joslin "Use of Ultrasound with Motion Capture to Measure Bone Displacement during Movement made for Functional Hip Joint Center Determination" *CMBES / APIBQ Joint Conference*, May 21-24, 2013